US Army Corps of Engineers

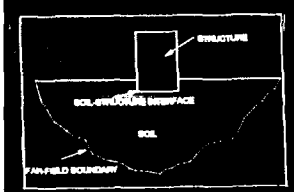

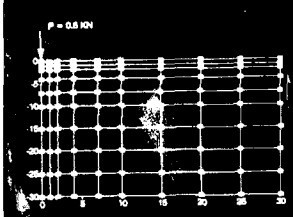

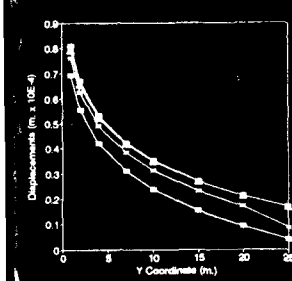

TECHNICAL REPORT ITL-92-3

SOLUTION OF SOIL-STRUCTURE INTERACTION PROBLEMS BY COUPLED BOUNDARY ELEMENT-FINITE ELEMENT METHOD

by

T. Kuppusamy, Mark A. Zarco

Charles Via Department of Civil Engineering
Virginia Polytechnic Institute and State University
Blacksburg, Virginia 24061

and

Robert M. Ebeling

Information Technology Laboratory

DEPARTMENT OF THE ARMY
Waterways Experiment Station, Corps of Engineers
3909 Halls Ferry Road, Vicksburg, Mississippi 39180-6199

May 1992
Final Report

Prepared for DEPARTMENT OF THE ARMY
US Army Corps of Engineers
Washington, DC 20314-1000

Under Contract No. DACW39-91-C-0085

Destroy this report when no longer needed. Do not return it to the originator.

The findings in this report are not to be construed as an official Department of the Army position unless so designated by other authorized documents.

The contents of this report are not to be used for advertising, publication, or promotional purposes. Citation of trade names does not constitute an official endorsement or approval of the use of such commercial products.

REPORT DOCUMENTATION PAGE

Form Approved
OMB No. 0704-0188

1. AGENCY USE ONLY *(Leave blank)*	2. REPORT DATE	3. REPORT TYPE AND DATES COVERED
	May 1992	Final report

4. TITLE AND SUBTITLE

Solution of Soil-Structure Interaction Problems by Coupled Boundary Element-Finite Element Method

5. FUNDING NUMBERS

DACW39-91-C-0085

6. AUTHOR(S)

T. Kuppusamy, Mark A. Zarco, Robert M. Ebeling

7. PERFORMING ORGANIZATION NAME(S) AND ADDRESS(ES)

See reverse

8. PERFORMING ORGANIZATION REPORT NUMBER

Technical Report ITL-92-3

9. SPONSORING/MONITORING AGENCY NAME(S) AND ADDRESS(ES)

US Army Corps of Engineers
Washington, DC 20314-1000

10. SPONSORING/MONITORING AGENCY REPORT NUMBER

11. SUPPLEMENTARY NOTES

Available from National Technical Information Service, 5285 Port Royal Road Springfield, VA 22161.

12a. DISTRIBUTION/AVAILABILITY STATEMENT

Approved for public release; distribution is unlimited.

12b. DISTRIBUTION CODE

13. ABSTRACT *(Maximum 200 words)*

This report presents a substructure method for coupling the boundary element method (BEM) and the finite element method (FEM) in order to solve soil-structure interaction problems more accurately and efficiently so that the nonlinear effects can be included in the near field by FEM and the far field simulated by BEM. Linear boundary elements based on the Melan solution are coupled with bilinear isoparametric finite elements in a manner consistent with the variational formulation of the problem. The undesirable properties of the unsymmetry and fully populated nature of the stiffness matrix resulting from the boundary element method are minimized by renumbering the system of equations such that the degrees of freedom associated with the boundary element system are isolated and assembled by the substructure method.

The accuracy of the method is verified by solving typical elastic problems involving semi-infinite domains. A comparison of the results shows a significant increase in the accuracy of both the displacements and stresses predicted using the proposed method. It was noted that the

(Continued)

14. SUBJECT TERMS

Boundary element methods
Finite element method
Soil-structure interaction -- Mathematics

15. NUMBER OF PAGES

58

16. PRICE CODE

17. SECURITY CLASSIFICATION OF REPORT	18. SECURITY CLASSIFICATION OF THIS PAGE	19. SECURITY CLASSIFICATION OF ABSTRACT	20. LIMITATION OF ABSTRACT
UNCLASSIFIED	UNCLASSIFIED		

7. (Continued)

Virginia Polytechnic Institute and State University
Charles Via Department of Civil Engineering
Blacksburg, VA 24061

USAE Waterways Experiment Station, Information Technology Laboratory
3909 Halls Ferry Road
Vicksburg, MS 39180-6199

13. (Continued)

displacements and stresses obtained by using the finite element method alone resulted in errors of more than 20 percent in certain cases. In particular, it was noted that the horizontal normal stresses and shear stresses were in error by 50 percent. Using the proposed method, the displacements and stresses were within 2 percent of the analytical solution.

The proposed substructure method can easily be incorporated into an existing finite element program because it simply involves adding a new element to the existing element library and modifying the assembly procedure.

PREFACE

This report describes the procedure for soil-structure interaction analysis using the coupled finite element boundary element method. The work was performed by Mark Zarco, Ph.D., student at Virginia Tech, under the guidance of Dr. T. Kuppusamy, Professor of Civil Engineering, Virginia Tech. This work was funded by the U.S. Army Engineer Waterways Experiment Station (WES) under Contract No. DACW39-91-C-0085.

This report was prepared by Dr. Kuppusamy, Mr. Zarco, and Dr. Robert Ebeling, Scientific and Engineering Applications Center, Computer-Aided Engineering Division (CAED), Information Technology Laboratory (ITL), WES. The work was managed and coordinated by Dr. Reed L. Mosher, Interdisciplinary Research Group, CAED, ITL, and Dr. Ebeling. All the work was accomplished under the general supervision of Mr. Paul Senter, Chief, CAED, and Dr. N. Radhakrishnan, Director, ITL.

At the time of publication of this report, Director of WES was Dr. Robert W. Whalin. Commander and Deputy Director was COL Leonard G. Hassell, EN.

TABLE OF CONTENTS

CONVERSION FACTORS, NON-SI TO SI (METRIC) UNITS OF MEASUREMENT

Non-SI units of measurement used in this report can be converted to SI (metric) units as follows:

Multiply	By	To Obtain
feet	0.3048	metres
inches	2.54	centimetres
inches	0.0254	metres
pounds	4.4822	newtons
tons	8.896	kilonewtons
pounds per square foot	47.8803	pascals
pounds per square foot	0.04788	kilopascals
pounds per square inch	6.8948	kilopascals
tons per sqaure foot	95.76	kilopascals
tons per sqaure foot	0.976	kg/cm^2

SOLUTION OF SOIL-STRUCTURE INTERACTION PROBLEMS BY COUPLED BOUNDARY ELEMENT-FINITE ELEMENT METHOD

Introduction

Soil-Structure interaction problems in geotechnical engineering involve the solution of boundary value problems consisting of two domains, a finite domain representing the structure and a semi-infinite domain representing the soil into which the structure is embedded. These two distinct domains are separated by a boundary called the soil-structure interface. Figure 1 illustrates a typical soil structure interaction problem. The aim of solving the boundary value problem is to determine the displacements and stresses in both domains. In general, it is very difficult to obtain a closed form solution to the above problem and in most cases the solution must be obtained numerically. Recently, the finite element method has been widely applied to the solution of this class of boundary value problems. The main advantage of this method is its capability to solve nonlinear boundary value problems with arbitrary geometry, boundary conditions and constitutive properties. One limitation of this method however is that it can only solve finite domain problems. Thus, infinite domain problems are approximately solved by taking a considerably large domain and assuming the displacements vanish along the far-field boundary distant from the region of interest. More recently, the boundary element method has been used to solve such infinite domain problems. For linear problems, the boundary element method results in a smaller system of equations with much greater accuracy particularly in infinite and semi-infinite domain problems. One limitation of this method is that problems involving non-homogeneous and non-linear domains result in a more complicated solution procedure. A compromise between the two methods would be to model the non-linear and non-homogeneous domain in the near field region of interest using finite elements and to model the far-field boundary using boundary elements assuming that the distant domain is linear and homogeneous. The resulting problem is a coupled model involving both boundary element and finite element systems. The main setback in this approach is that the symmetry and bandedness of the system of equations resulting from the finite element method is destroyed by the boundary element method. Thus, the matrix resulting from the coupling of both systems is unsymmetric as well as fully populated. The purpose of this paper is to show that use of boundary elements for modeling the far field in the finite element analysis results in a significant improvement in accuracy and such a technique can be efficiently implemented.

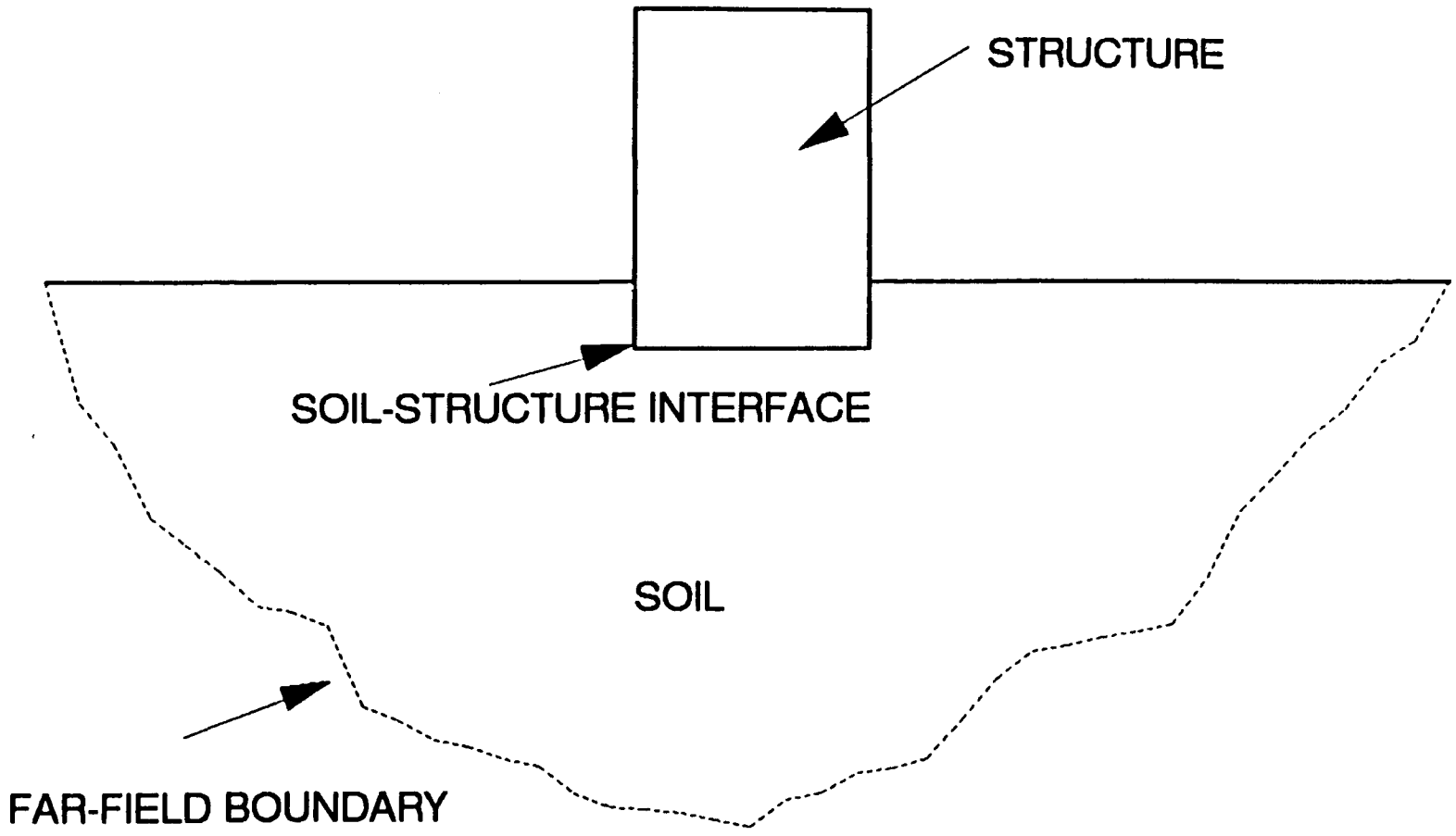

Figure 1 A Typical Soil-Structure Interaction Problem

Boundary Element Method

The direct boundary element method is a numerical technique for solving boundary value problems. In this method, the governing differential equations are converted into an equivalent integral statement by successively applying the divergence theorem. This integral statement, called the *boundary integral equation*, for an elastostatic boundary value problem is given by (Brebbia [1984])

$$C_{ij}(s)u_j(s) + \int_{\Gamma} p^*_{ij}(s,q)\, u_j(q)d\Gamma = \int_{\Gamma} u^*_{ij}(s,q)\, p_j(q)d\Gamma \tag{1}$$

The displacements and tractions $u_j(q)$ and $p_j(q)$, are the jth component at point q on the boundary Γ. The displacements and tractions $u^*_{ij}(s,q)$ and $p^*_{ij}(s,q)$, are the fundamental solution corresponding to the jth component at point q due to a unit force applied at point s in the ith direction where both points s and q are on the boundary Γ and $C_{ij}(s)$ is a 2×2 matrix which is a function of the point s.

The basic steps in the boundary element method involve:

(a) The boundary Γ is discretized into a series of elements of which displacement and tractions are chosen to be piecewise interpolated between the element nodal points;

(b) The boundary integral equation is applied in discretized form to each nodal point s on the boundary Γ and the integrals are computed (usually by a numerical quadrature scheme) over each boundary element. A system of N linear algebraic equations involving the set of N nodal tractions and N nodal displacements is therefore obtained;

(c) Boundary conditions are imposed and consequently N nodal values (traction or displacement in each direction per node) are prescribed. The system of N equations can therefore be solved by standard methods to obtain the remaining boundary conditions.

In what follows, each of the above steps shall be explained more thoroughly together with an application to the solution of two dimensional elastostatic problems using linear elements.

For the discretization of the boundary integral equation, the boundary Γ is approximated by using a series of elements. The Cartesian coordinates (x,y) of points located within each element Γ_i are expressed in terms of the lagrangian interpolating functions ψ_j and the nodal coordinates (x_j, y_j) of the element by the following relation

$$x = \sum_{j=1}^{n} x_j \psi_j \qquad y = \sum_{j=1}^{n} y_j \psi_j \tag{2}$$

Similarly, the boundary displacements and tractions are approximated over each element in terms of the lagrangian interpolating function ψ_j in the following relation

$$u_i = \sum_{j=1}^{n} U_{ij} \psi_j \qquad p_i = \sum_{j=1}^{n} P_{ij} \psi_j \tag{3}$$

where u_i and p_i is the ith component of the displacements and tractions along the element and U_{ij} and P_{ij} is the ith component of the nodal tractions.

Assuming that the boundary Γ is discretized into L elements Γ_j, the substitution of the above approximations into eqn. (1) results in matrix form

$$C(s_i)u(s_i) + \sum_{j=1}^{n}\left(\int_{\Gamma_j} p^*(s_i,q)\, \psi d\Gamma \right) U(q) \;\; = \sum_{j=1}^{n}\left(\int_{\Gamma_j} u^*(s_i,q)\psi d\Gamma \right) P(q) \tag{4}$$

for a boundary node s_i .

In general, the integrals presented in the above equation must be computed numerically. However, for the case when the singular node i lies within the element Γ_j, the integral becomes improper because of the singularity in both p^* and u^*. The special treatment of theses integrals shall be described later. For the case when the singular points is outside the element Γ_j the integral can be readily replaced by

$$\int_{\Gamma_j} p^* \, \psi \, d\Gamma = \int_{-1}^{1} p^* \, \psi \, |J| \, d\eta = \sum_{k=1}^{K} |J|_k W_k (p^* \psi)_k \tag{5}$$

$$\int_{\Gamma_j} u^* \, \psi \, d\Gamma = \int_{-1}^{1} u^* \, \psi \, |J| \, d\eta = \sum_{k=1}^{K} |J|_k W_k (u^* \psi)_k \tag{6}$$

where K is the number of Gaussian integration points, W_k is the weighting factor associated with them, η is the local coordinate system and $|J|$ is the Jacobian of the transformation given by

$$|J| = \sqrt{\left(\frac{dx}{d\eta}\right)^2 + \left(\frac{dy}{d\eta}\right)^2} \tag{7}$$

Application of eqn. (4) to all nodes results in a system of equations of the form

$$(C + H)U = GP \tag{8}$$

or

$$\hat{H}U = GP \tag{9}$$

where $\hat{H} = C + H$ and C is a diagonal matrix consisting of the constants $C(s_i)$ mentioned previously.

For the special case when the point s_i is one of the nodal points of the element Γ_i, the right-handside term involving u^* must either be integrated analytically as is possible for constant and linear elements (Brebbia [1978] and [1984], Crouch [1983]), or for higher order elements, the logarithmic part must be separately integrated using a special numerical quadrature (Cristescu [1978]). Other methods involve developing techniques where the singular terms cancel (Zeng [1990]).

It should be noted that for the total computation of $\hat{H}$, the leading diagonal submatrices which correspond to the term C_{ij}, the principal value of the integral in eqn. (4) can be calculated by imposing to the matrix equation the condition that rigid body translations result in zero tractions. Thus result of this is that for eqn. (9), $\hat{H}$ can be computed using the following relations (Brebbia [1978])

$$\hat{H}_{\alpha\alpha} = -\sum_{q \neq \alpha}^{NN} H_{\alpha q} \tag{10}$$

for finite bodies and

$$\hat{H}_{\alpha\alpha} = I - \sum_{q \neq \alpha}^{NN} H_{\alpha q} \tag{11}$$

for infinite and semi-infinite domains. In the above expressions H_{ij} refers to a 2×2 submatrix corresponding to the evaluation of the fundamental solution at nodes i and j and I is a 2×2 identity matrix.

Fundamental Solution

For a general two dimensional plane strain elastostatic boundary value problems, the fundamental solution associated with a unit load applied at a point s within infinite plane, the

displacements and tractions at point q are given by (Timoshenko [1970])

$$u^*_{ij}(s,q) = \frac{-1}{8\pi(1-\nu)G}\left\{(3-4\nu)\ln(r)\,\delta_{ij} - \frac{r_i\,r_j}{r^2}\right\}$$

$$p^*_{ij}(s,q) = \frac{-1}{4\pi(1-\nu)r}\left\{\left[(1-2\nu)\,\delta_{ij} + 2\,\frac{r_i r_j}{r^2}\right]\frac{\partial r}{\partial n} - (1-2\nu)\left(\frac{r_i n_j - r_j n_i}{r}\right)\right\}$$

where the subscripts i and j refer to the directions of the applied unit force and the resulting component of the corresponding quantity respectively. Also,

$$\delta_{ij} = \begin{cases} 0 \text{ for } i \neq j \\ 1 \text{ for } i = j \end{cases}$$

and where r is the distance between points s and q, r_i is the ith component of r and n is the unit vector normal to the boundary Γ at point q, and ν is the Poisson's ratio. In most boundary element literature, this solution if referred to as the Kelvin solution. The above fundamental solution is suitable for solving both finite and infinite domain problems. For soil-structure interaction problems however, there is a need to model the far field as an infinite half-plane. The fundamental solution corresponding to this problem was obtained by Melan [1932]. However, in the original work, there seem to be errors which were pointed out by Telles [1981]. The analytical solution to this problem consists of superposing a complementary solution $(\,)^*_c$ on the Kelvin solution $(\,)^*_k$. Thus the solution can be expressed as

$$u^* = u^*_k + u^*_c$$

$$p^* = p^*_k + p^*_c$$

The complete and correct expression for the complementary solution is given in Appendix B. In the proposed solution procedure, the Melan fundamental solution is used to account for the semi-infinite far field domain. This aspect of the procedure contrasts with other researchers, Vallabhan [1986] and Georgiou [1981] for example, who use the Kelvin fundamental solution in their boundary element procedure to model the far field. It should be pointed out that the result of adopting the Kelvin solution is that the far field domain must be treated as a large finite body and the displacements must be assumed to vanish as points away from the region of interest are considered.

Linear Boundary Elements

Among the different types of elements that can be employed in the numerical disretization of the boundary integral equation, the linear element has been found to give acceptable accuracy without

requiring much computer effort for the solution of the examples presented here. The geometry of the element is represented by a straight line of length l and $|J| = l/2$. Also the interpolating functions are given by

$$\psi_1(\xi) = \frac{(1-\xi)}{2} \qquad \psi_2(\xi) = \frac{(1+\xi)}{2} \tag{12}$$

It can be seen that the discretization of the boundary integral equation gives rise to two element matrices h and g (corresponding to H and G respectively) of order 2×4 in the following form

$$h = \frac{l}{2} \int_{-1}^{1} [p^* \psi_1 \;\; p^* \psi_2] d\eta \tag{13}$$

$$g = \frac{l}{2} \int_{-1}^{1} [u^* \psi_1 \;\; u^* \psi_2] d\eta \tag{14}$$

For the special case where the singular node is coincident with one of the end nodes of the element, the coefficients of the g matrix can be computed analytically to avoid significant error introduced by numerical integration of the improper integral. For the Kelvin solution, the following expression is obtained

$$g_{ij}^{kn} = \frac{1}{[16\pi(1-\nu)G]} \left\{ (3-4\nu) l \; [\delta_{kn} + 0.5 \; - \ln(l)] \delta_{ij} + \frac{l_i \, l_j}{l} \right\}$$

for the half-plane solution, the complementary part is given by

$$g_{ij}^{kn} = \frac{1}{[4\pi G]} \left\{ 2(1-\nu) l \; [\delta_{kn} + 0.5 \; - \ln(l)] \delta_{ij} + \frac{l_i \, l_j}{l} + \alpha (1-\delta_{ij}) l \; \theta \; (1-2\nu) \right\}$$

where the subscripts i and j indicate the position of the coefficient in the 2×2 submatrix k of g and n indicates the singular node. Also

$$\delta_{ij} = \begin{cases} 0 \text{ for } i \neq j \\ 1 \text{ for } i = j \end{cases}$$

$$\alpha \;\; = \begin{cases} -1 \text{ for } j = 1 \\ 1 \text{ for } j = 2 \end{cases}$$

$$\theta = \arctan(l_2/l_1) \qquad (-\pi/2 \leq \theta \leq \pi/2)$$

and where l_i is the ithe component of the element length.

Coupling the Boundary-Finite Element System

For an elastostatic boundary value problem, the system of linear equations resulting from the finite element method can be written in the form

$$KU = F \tag{15}$$

where K is the stiffness matrix, u is the vector of nodal displacements, and F is the vector of nodal forces. The resulting system of equations resulting from the boundary element method can be expressed in the form

$$\hat{H}\underline{U} = G\underline{P} \tag{16}$$

where H and G are the matrices of influence coefficients, $\underline{u}$ is the vector of nodal displacements, and $\underline{p}$ is the vector of nodal tractions in the boundary element system. The nodal traction can be converted into equivalent nodal forces using an appropriate definition of the form

$$N\underline{P} = \underline{F} \tag{17}$$

where N is a square transformation matrix which converts the nodal tractions to equivalent nodal loads. Using the above definitions, the modified boundary element system is of the form

$$\hat{H}\underline{U} = GN^{-1}\underline{F} \tag{18}$$

which can be rewritten as

$$\hat{K}\underline{U} = \underline{F} \tag{19}$$

where

$$\hat{K} = G^{-1}N\hat{H} \tag{20}$$

To describe the procedure, assume that the finite element system can be partitioned into those

nodes which are included only in the finite element system, and those nodes common to both the finite element and boundary element system. The partitioned system of equations thus can be written as

$$\begin{bmatrix} K_{ff} & K_{fb} \\ K_{bf} & K_{bb} \end{bmatrix} \begin{bmatrix} U_f \\ U_b \end{bmatrix} = \begin{bmatrix} F_f \\ F_b \end{bmatrix} \tag{21}$$

where u_b and F_b are the displacements and nodal forces respectively lying on the interface of the finite element and boundary element domains while u_f and F_f are the displacements and nodal forces respectively not lying on the finite element and boundary element interface.
The boundary element system can be written as

$$\hat{K}\underset{\sim}{U} = \underset{\sim}{F} \tag{22}$$

The variables in the two systems are related by continuity and equilibrium which require that

$$U_b = \underset{\sim}{U} \tag{23}$$

$$F_b + \underset{\sim}{F} = 0 \tag{24}$$

or

$$\underset{\sim}{F} = -F_b \tag{25}$$

Thus, applying the conditions mentioned in Eqns. (9) and (10) yield the coupled system of the form

$$\begin{bmatrix} K_{ff} & K_{fb} \\ K_{bf} & K_{bb} + \hat{K} \end{bmatrix} \begin{bmatrix} U_f \\ U_b \end{bmatrix} = \begin{bmatrix} F_f \\ 0 \end{bmatrix} \tag{26}$$

It should be noted that the stiffness matrix K is symmetric positive definite and banded while the stiffness matrix for the modified boundary element method $\hat{K}$ is non-symmetric and fully populated. Thus, because of the boundary element coupling, the symmetry and bandedness of the stiffness matrix in the finite element method is lost.

Some researchers (Vallabhan [1986], Georgiou [1981]) have tried to retain the symmetry of the stiffness matrix by developing an approximate stiffness matrix for the modified boundary element method. One way of doing this is by taking only the symmetric part of the matrix and discard the

skew-symmetric part. Thus the approximate stiffness matrix is given by

$$\hat{k}^S_{ij} = \tfrac{1}{2}(\hat{k}_{ij} + \hat{k}_{ji}) \tag{27}$$

where k_{ij} is the (i,j)th element of the $\hat{K}$ matrix.

In the process of this research, the effect of discarding the skew-symmetric portion of the $\hat{H}$ and G matrix on the accuracy of the solution was investigated. This consisted of solving typical elasticity problems using both the unsymmetric and symmetric $\hat{H}$ and G matrices in the boundary element solution. Results from this investigation indicate that if the Kelvin solution is used and the problem is solved without taking advantage of the geometric symmetry of the problem, there is no significant effect due to discarding the skew-symmetric part. However, if geometric symmetry is taken into account by reflecting the singular nodes, significant errors occur. If the Melan solution is used, it was determined that the error due to discarding the skew-symmetric part is dependent upon the value assigned to poisson's ratio ν. That is, as ν approaches 0.5, the error increases regardless of whether or not symmetry is taken into account. It should be noted however that when the boundary element method is coupled with the finite element method in the procedure described above, the effects of discarding the skew-symmetric part on the accuracy of the final results are minimized. There are two reasons for this. First, because the elements of the boundary element stiffness matrix derived in eqn. (20) are considerably smaller that the finite element stiffness matrix into which they are assembled and thus the symmetry of the finite element matrix decreases the ratio of the skew-symmetric part over the symmetric part of the overall stiffness matrix. Secondly, it was observed that because the transformation matrix N is symmetric, the resulting stiffness matrix $\hat{K}$ is more symmetric than that corresponding to the boundary element method alone and given by

$$\widetilde{K} = G^{-1}\hat{H} \tag{28}$$

The coupling procedure can be summarized in to the following steps:

STEP 1: From the problems geometry and material parameters given form the $\hat{H}$, G and N matrices. The formulation of the N matrix is given in Appendix C.

STEP 2: Perform the matrix operations specified in eqn. (20) to obtain the boundary element stiffness matrix $\hat{K}$.

STEP 3: If only the symmetric part of $\hat{K}$ is to be used, discard the skew-symmetric part using the

procedure described in eqn. (27).

STEP 4: Assemble the stiffness matrix $\widehat{K}$ into the global stiffness matrix.

STEP 5: Solve the resulting system of equations as would be done for a purely finite element system. However, if the full $\widehat{K}$ is used, an usymmetric solution technique must be used.

STEP 6: Using the displacements, compute the stresses as would be done in a purely finite element system.

It should be noted from the above discussion that once the equivalent stiffness matrix for the boundary element system is obtained it can be assembled into the finite element system in the same way finite elements are assembled. Thus, the coupling procedure proposed can be viewed as treating the boundary element system as a substructure and obtaining the stiffness matrix corresponding to this substructure. The substructure is treated as a special finite element which can be incorporated into the element library of an exiting finite element program. In order to obtain a system of equations where the degrees of freedom common to both the finite element and boundary element system occur as described in eqn. (26), a procedure of renumbering the equations is used. The process of renumbering is described in greater detail in the following section. The main purpose in separating these degrees of freedom is to minimize the band width that comes from the dense nature of the substructure's stiffness matrix.

Program Implementation

A coupled boundary element-finite element program BEFEC was developed to verify the validity of the proposed coupling technique. The finite element portion of BEFEC was derived from static portion of DLEARN, a program developed by Hughes [1988]. The boundary element portion was derived from the elastostatic 2D program developed by Brebbia [1984] and contains additional features such as the half-plane fundamental solution. The system of equations are assembled into an active column form where only the non-zero quantities in the global stiffness matrix occurring beneath the skyline are stored. The scheme of storage is one of the most efficient in terms of amount of memory used as well as computer time required. The only modification in the algorithm used to assign the equations numbers is that two passes instead of one are used. In the first pass, equation numbers are assigned to those degrees of freedom corresponding to nodes which are not on the far field boundary. In the second pass, the nodes corresponding to the far field boundary are assigned equation numbers. This algorithm assures that the fully populated boundary element stiffness matrix is confined to the last

equation and prevents these terms from dispersing throughout the entire stiffness matrix. The result is that the column heights are minimized. The program also has the option to discard the skew-symmetric portion of the boundary element stiffness matrix thus resulting in an approximate symmetric boundary element stiffness matrix as done in eqn. (27). Vallabhan [1986] suggests the following condition be satisfied before discarding the skew symmetric part in order that the resulting error not be significant

$$\text{maximum} \left\{ \left\| \frac{a_{ij} - a_{ji}}{a_{jj}} \right\| \right\} \leq 0.01 \qquad \forall\ (i,j) \tag{29}$$

where a_{ij} are the elements of the global stiffness matrix. It was noted that in the problems considered, the above norm was much less than 1%. Vallabhan [1986] states that the above norm becomes smaller as the size of the problem increases.

It should be noted that in the solution of soil-structure interaction problems, while similar in many ways, the above solution procedure has three major differences from previously developed coupling techniques to solve such problems (Vallabhan [1986], Georgiou [1981]). First, the far field domain is modeled using boundary elements based on the half-plane (Melan) solution. This approach has be commonly used in dynamic soil structure interactions problems (Manolis[1988], Wolf[1988]). However, this is not so in the static case where the far field domain is modeled as a large finite body using boundary elements based on the infinite plane (Kelvin) solution. Also, in the works cited, constant boundary elements are used as compared to the linear boundary element used in the current formulation. Lastly, in the works cited, no renumbering is performed on the system of equations, making it necessary to store the full system of equations making the solution procedure costly in terms of memory required. It should also be stressed that many existing finite element programs use the active column storage scheme. Thus the proposed coupling technique can easily be integrated into such program since it merely involves adding a new element to the existing element library of these programs.

Program Validation

To validate the proposed solution method, two linear elastic half-plane problems were solved. For each problem, five different analyses were performed. This involved first conducting a finite element analysis using a suitable mesh and assuming the far field displacements vanish. A second finite element analysis was conducted using an expanded domain while retaining the same refinement as the first analysis. A third finite element analysis was conducted using the same domain as the first analysis but more refined mesh. Two coupled boundary element-finite element analyses were conducted using the same mesh as in the first finite element analysis but modeling the far field effects using boundary

elements. In the first coupled analysis the unsymmetric part of the stiffness matrix resulting from the boundary element method was considered while the analysis neglected this part of the stiffness matrix.

Problem 1: This problem consists of a concentrated load applied to a half space. To solve this problem, four different analyses were considered namely: (1) a finite element analysis consisting of a 30 m. × 3.0 m. region using 100 nodes and 81 elements, FEM (100) [fig. 2] , (2) a finite element analysis consisting of a 60 m. × 60 m. region using 169 nodes and 144 finite elements, FEM (169A) [fig. 3], (3) a finite element analysis consisting of a 30 m. × 30 m. region using 169 nodes and 144 finite elements, FEM (169B) [fig. 4], and (4) a coupled boundary element/finite element analysis consisting of a 30 m. × 30 m. region with 100 nodes and 81 elements together with 18 boundary elements (BEFEC-18/100) and a symmetric solution (BEFEC2-18/100) where the skew-symmetric portion of the stiffness matrix was discarded. Symmetry of geometry was considered. The material properties were E=3.0 MPa, $\nu = 0.25$. The load applied had a magnitude of 0.5 KN. The complete analytical solution is given is Appendix A. In comparing the results of the numerical analysis with the analytical solution, the following observations are made.

1. Vertical Displacements Along the Centerline $u_y(x = 0, y)$: The initial finite element analysis FEM (100) shows a significant underprediction of the displacements (see fig. 5). No significant improvement is obtained by refining the mesh as can be seen from the results of FEM (169B). A substantial improvement is obtained when the domain of the problem is increased as shown by the results of FEM (169A). Results of the proposed technique show a very good agreement with the analytical solution. It is also observed that there is practically no difference between the unsymmetric and symmetric solution.

2. Horizontal Displacements Along the Surface $u_x(x, y = 0)$: Evaluating the analytical solution, it can be seen that the horizontal displacements along the surface are equal to a constant.

$$u_x|_{y=0} = \frac{-P_y(1-2\nu)}{4G}$$

Because the boundary conditions are assumed to vanish away from the load area, all three finite element solutions give answers which diverge from the analytical solution while both the coupled solutions are give much better answers which more closely agree with the analytical solution as can be seen in fig, (6) .

3. Vertical displacements along the surface. Results presented in fig. (7) show that like the

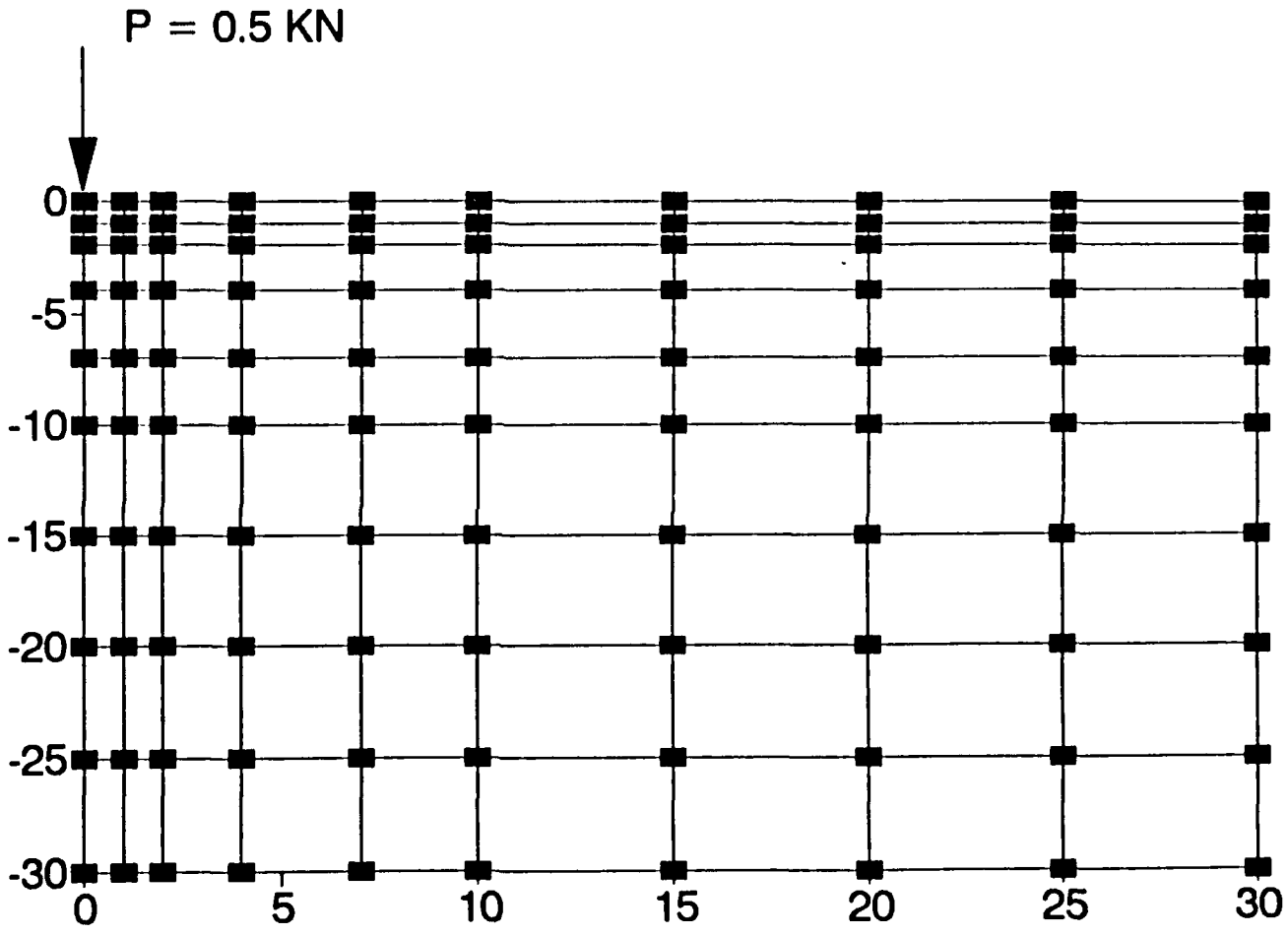

Fig. 2 FEM (100) Mesh

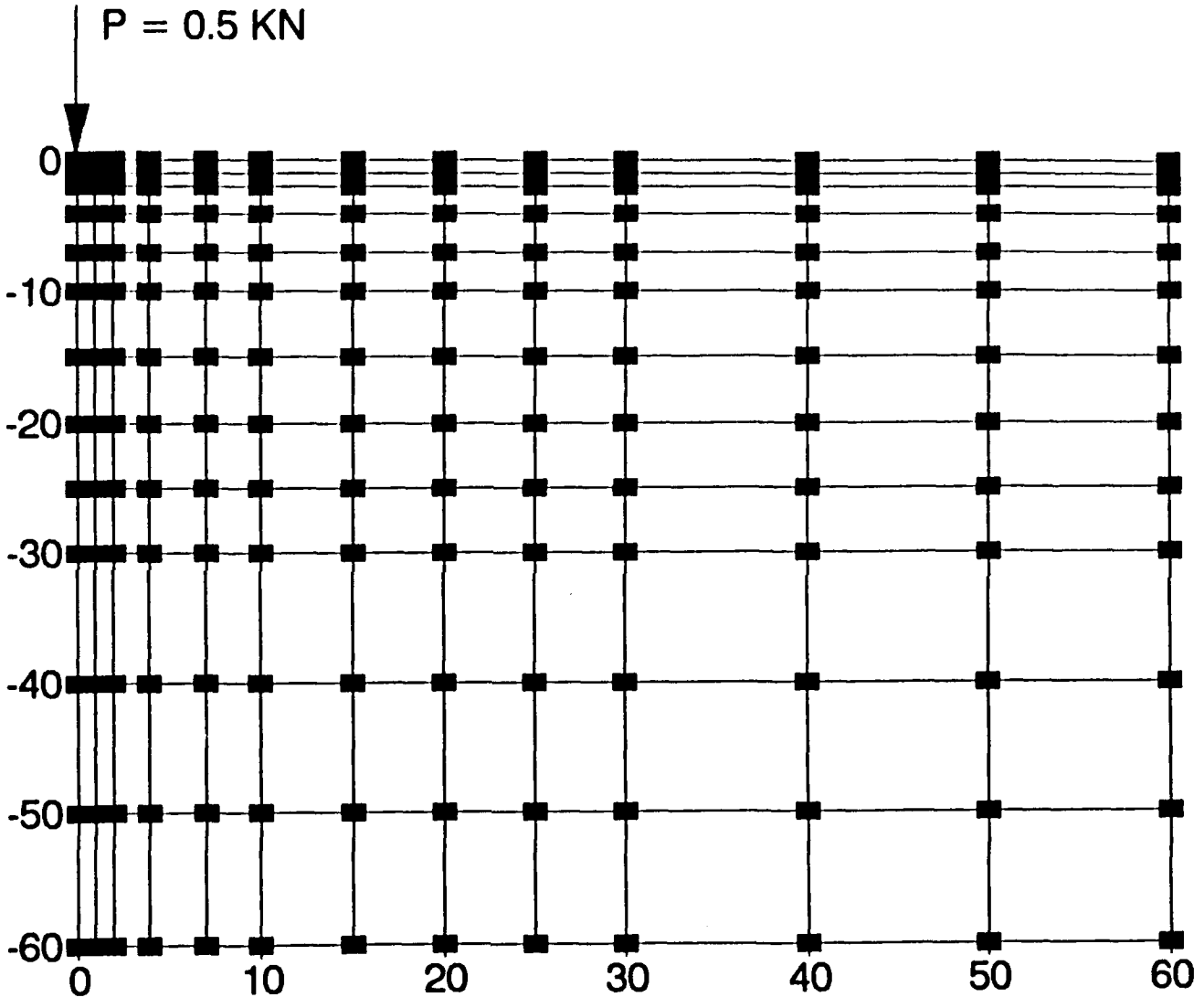

Fig. 3 FEM (169A) Mesh

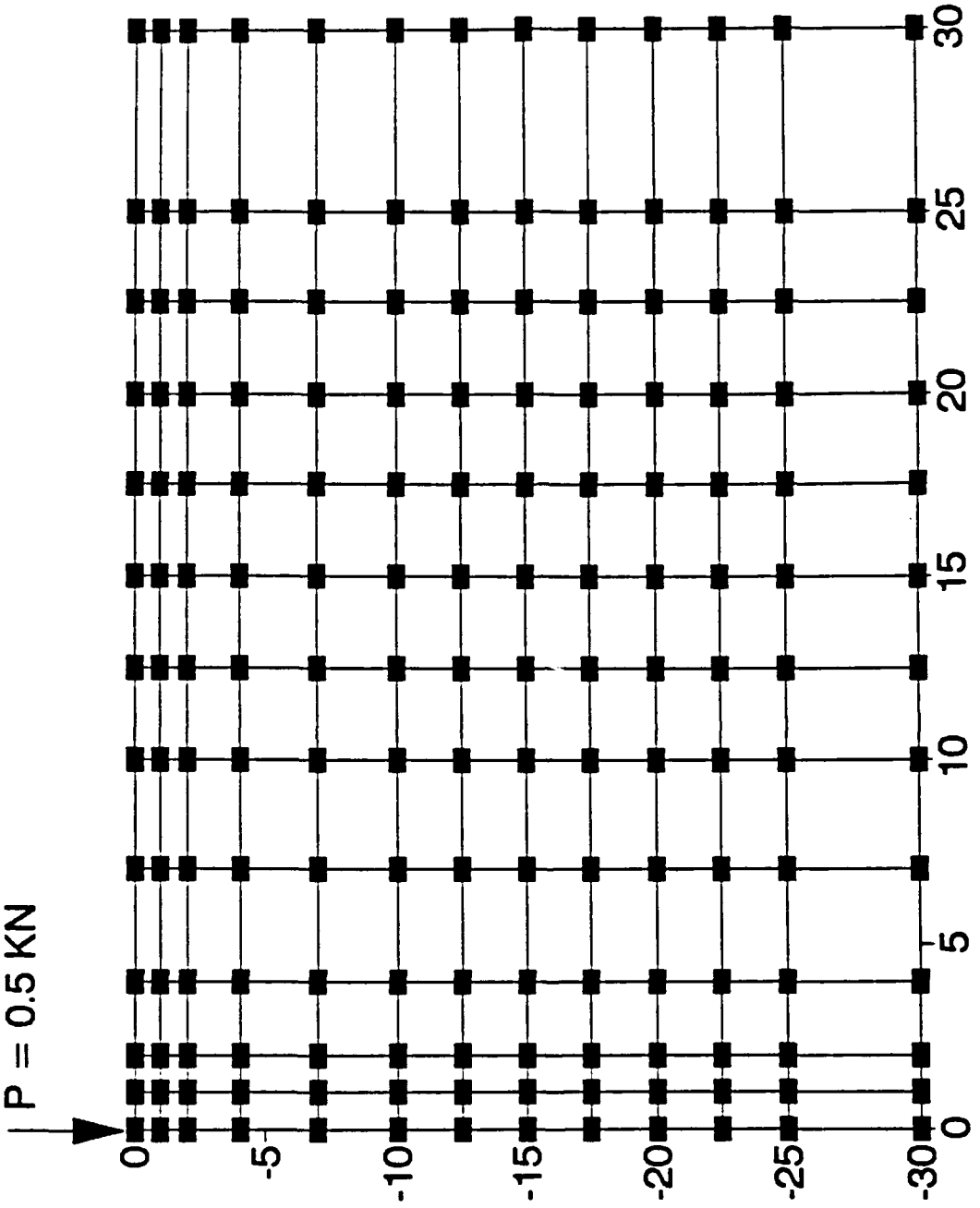

Fig. 4 FEM (169B) Mesh

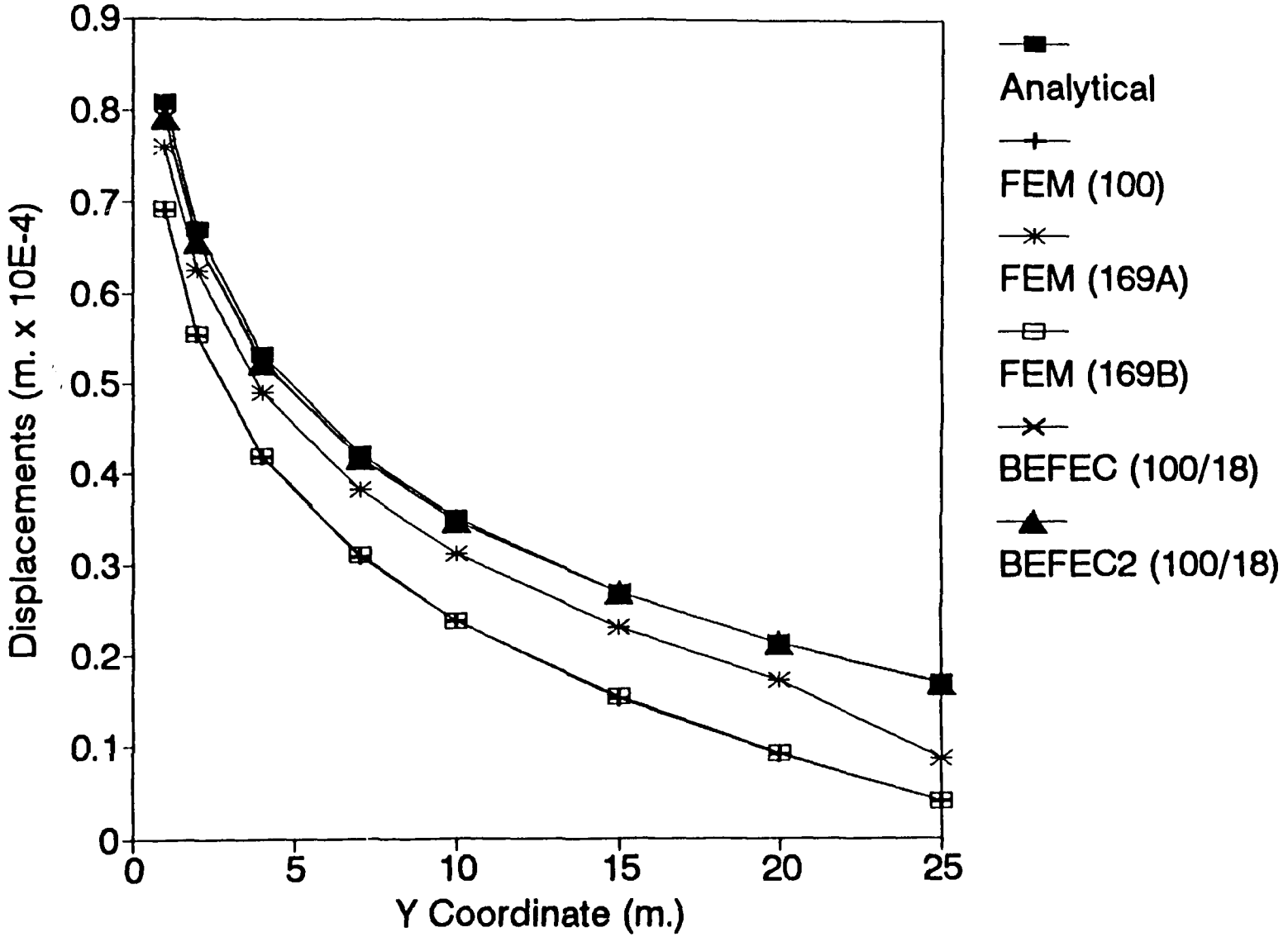

Fig. 5 Problem 1: Vertical Displacements Along Centerline

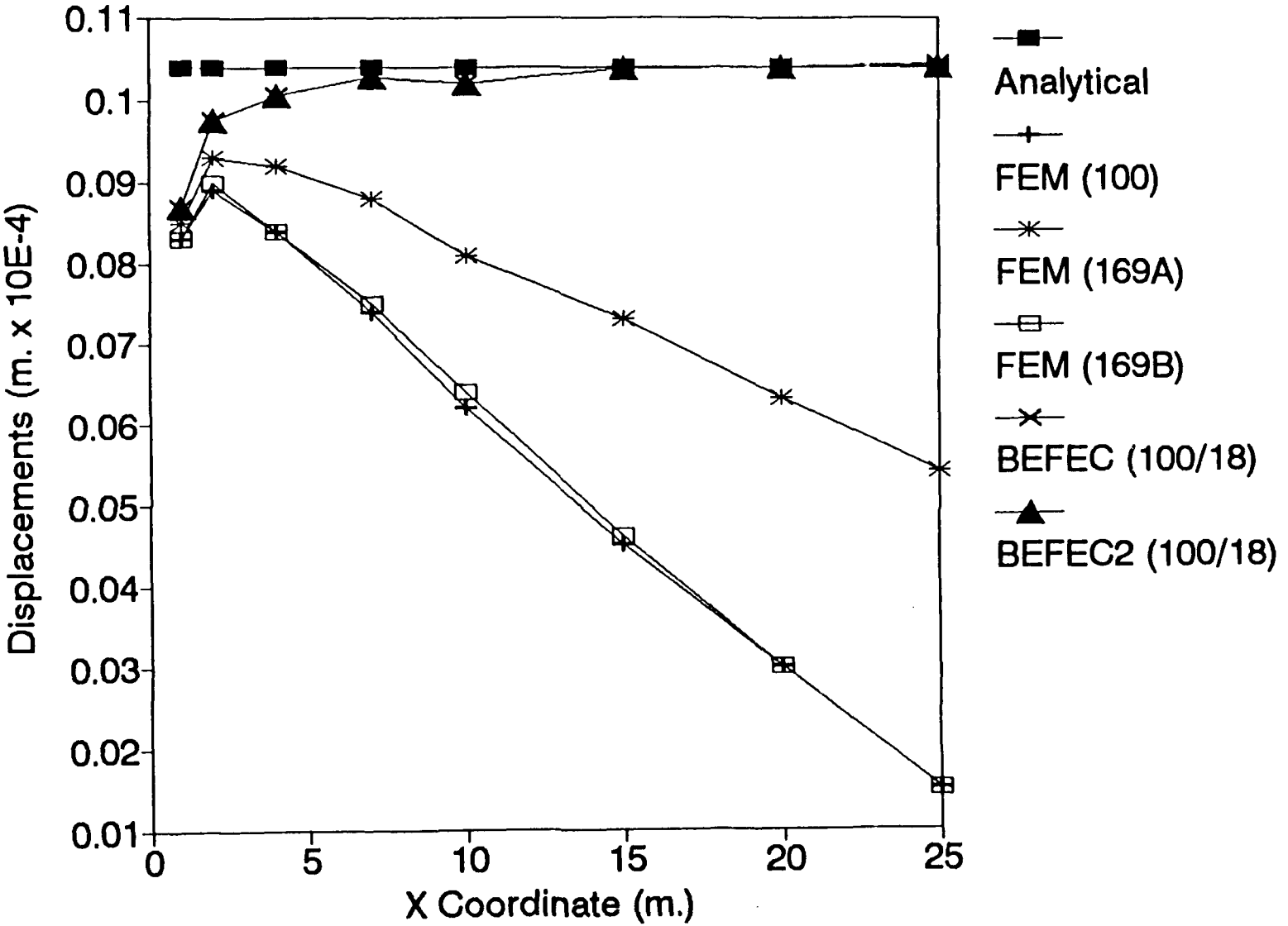

Fig. 6 Problem 1: Horizontal Displacements Along Surface

displacements along the centerline, the conventional method of finite element analysis FEM (100) results is a substantial disparity between the analytical and numerical solution. This disparity is little affected by refining the mesh as was done in FEM (169B). The prediction of vertical displacements can however be improved by coupling the solution with the boundary element method BEFEC (100/18) and BEFEC2 (100/18), or increasing the domain of the problem as in FEM (169A). In this particular case, the displacements obtained using the former procedure are much more accurate than those using the coupled solution. Almost no difference was noticed between the symmetric and unsymmetric solutions.

4. Horizontal Normal Stresses (σ_{xx}) along the diagonal elements. From fig (8) it can be seen that the stresses predicted by the finite element method alone FEM (100) and FEM (169A) are substantially underpredicted. It also can be seen that increasing the mesh size decreases the amount by which the stresses are underpredicted as is seen by the difference between two analyses. In comparison, except for points near the loaded area where the effects of stress concentration are dominant, both coupled solutions agree very well with the analytical solution. To further study the error involved in the stresses computed using the different methods of analysis, the relative error was ploted versus the x-coordinate in fig. (9). the relative error is defined as follows

$$\text{relative error } (\%) = \left|\frac{\sigma^a - \sigma^n}{\sigma^a}\right| \times 100\% \tag{30}$$

where σ^a is the analytical solution and σ^n is the numerical solution. It can be seen that except for the loaded area ($x < 2.5$ m.), the coupling method yields stresses which are well within 2% of the analytical solution while the finite element analysis alone yields errors of as much as 35% in both analyses indicating that the prediction is not improved by expanding the mesh size.

5. Shear Stresses (σ_{xy}) along the diagonal elements. Results of the analyses performed are presented in fig. (10). From the graph, it can be seen that the stress prediction by finite element method alone is reasonably accurate. Expanding the mesh as in FEM (169A) or coupling with the boundary element method as in BEFEC (100/18) and BEFEC2 (100/18) have no visible effect on the resulting solution indicating that these methods are convergent with respect to the accuracy of the solution. However, upon comparing with the relative error as presented in fig. (11), it can be seen that the far field solution is grossly in error. In particular, an underprediction of 68% occurs in the initial finite element solution FEM (100). This error is substantially reduced to 20% by expanding the mesh to twice the initial size as in FEM (169A). The results obtained using both the unsymmetric BEFEC (100/18) and symmetric BEFEC2 (100/18) coupled solution yield identical values within 2% of the analytical solution.

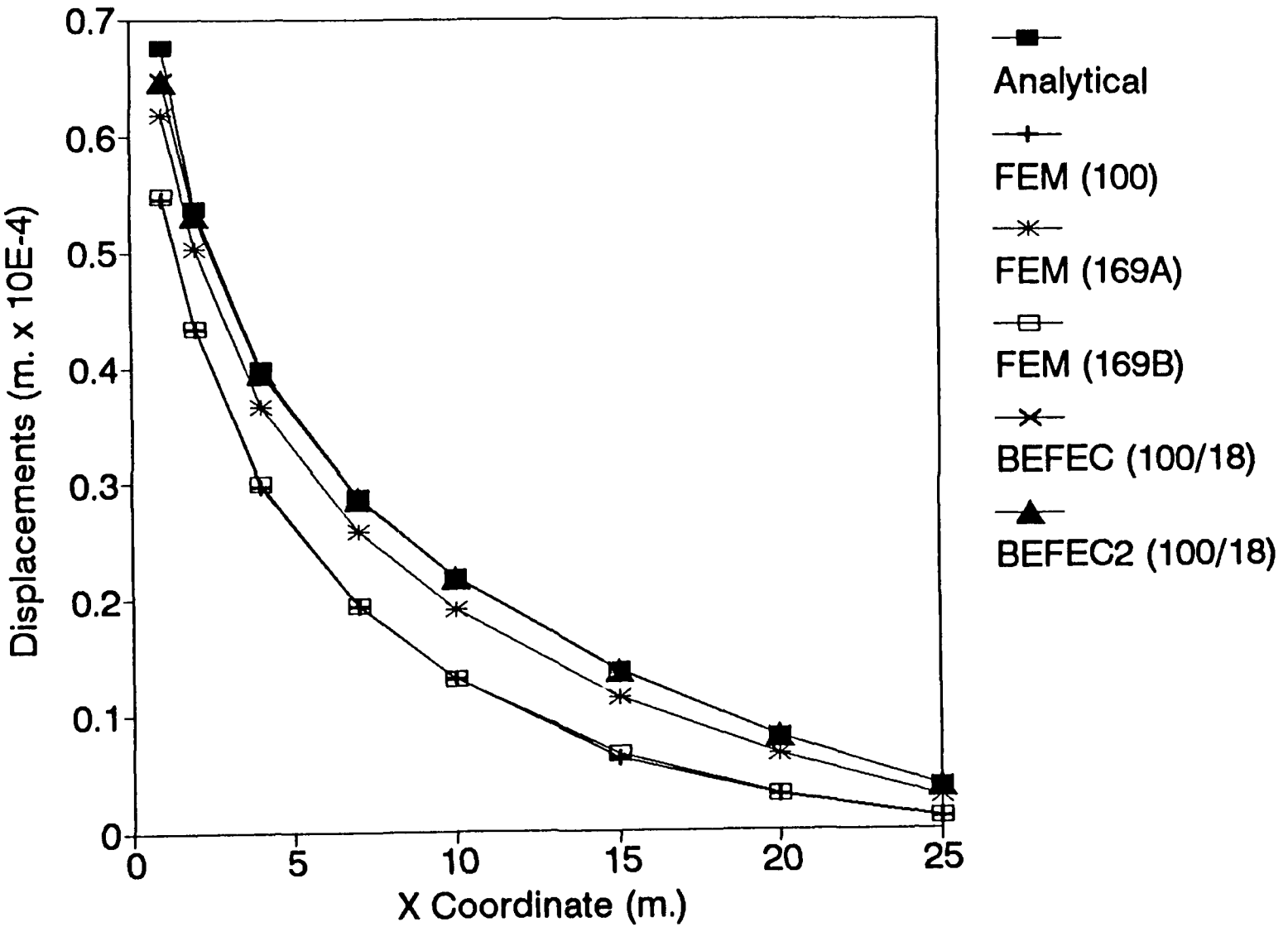

Fig. 7 Problem 1: Vertical Displacements Along Surface

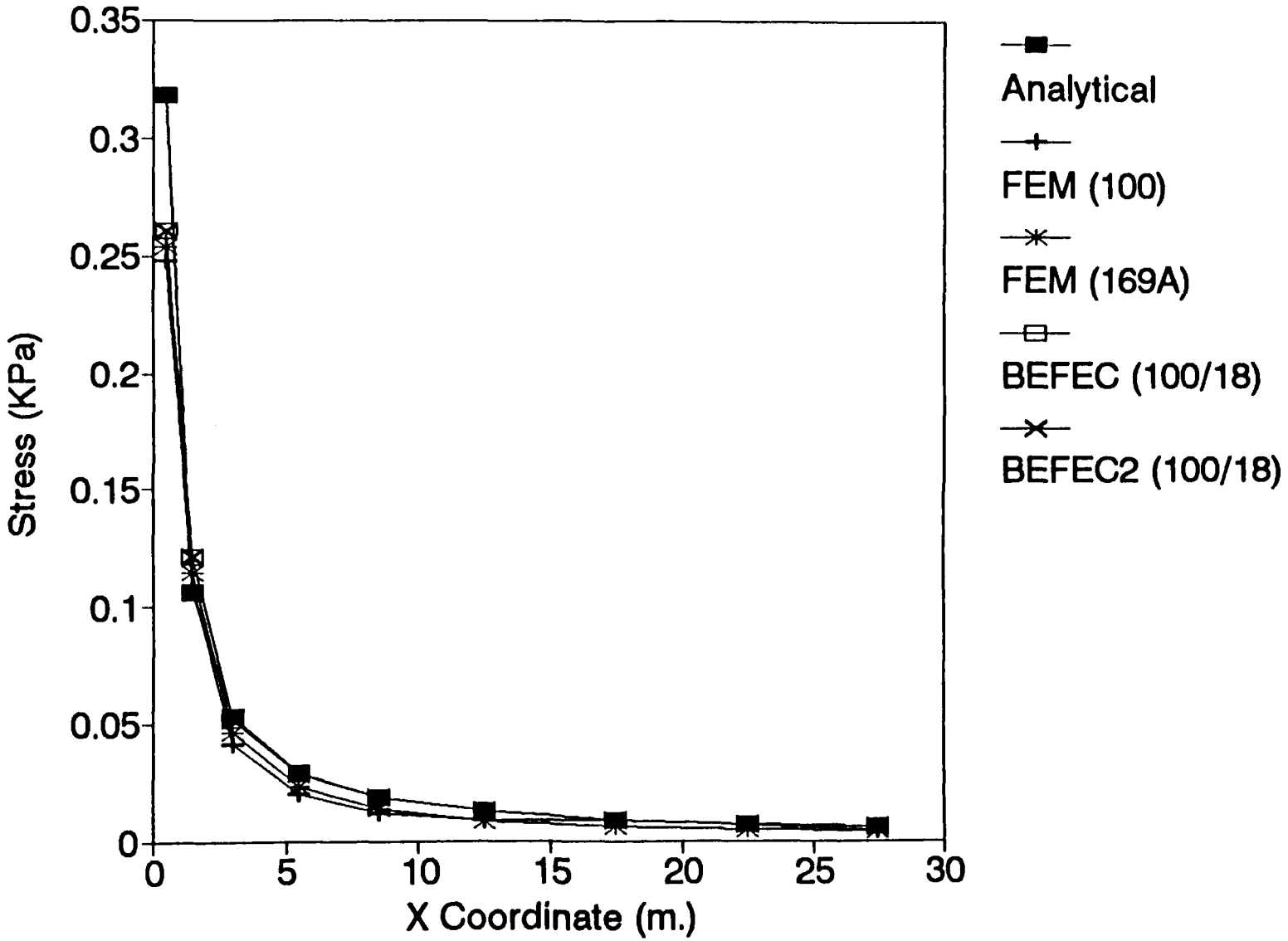

Fig. 8 Problem 1: Sigma-XX Along Diagonal Elements

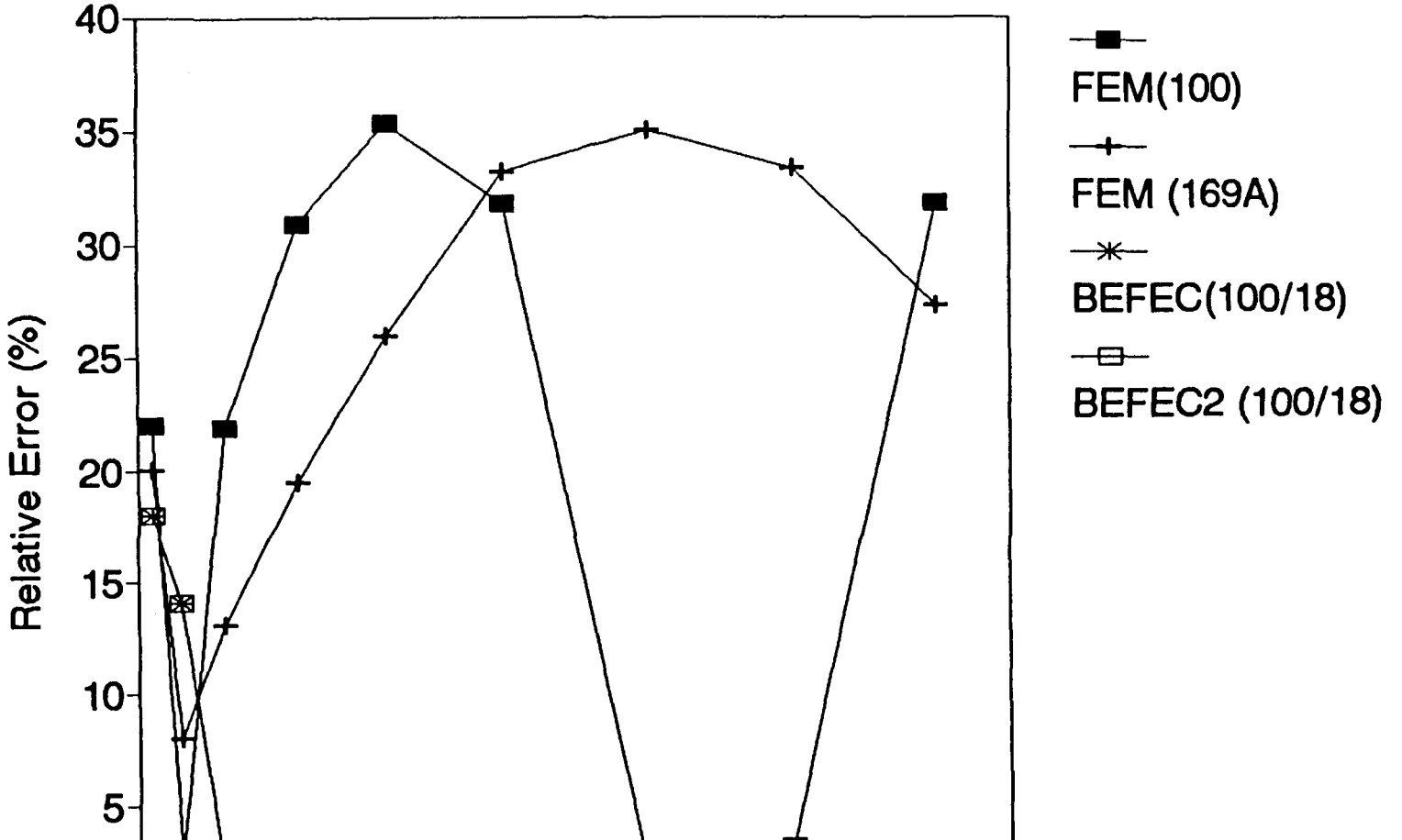

Fig. 9 Problem 1. Error in Sigma-XX Along Diagonal Elements

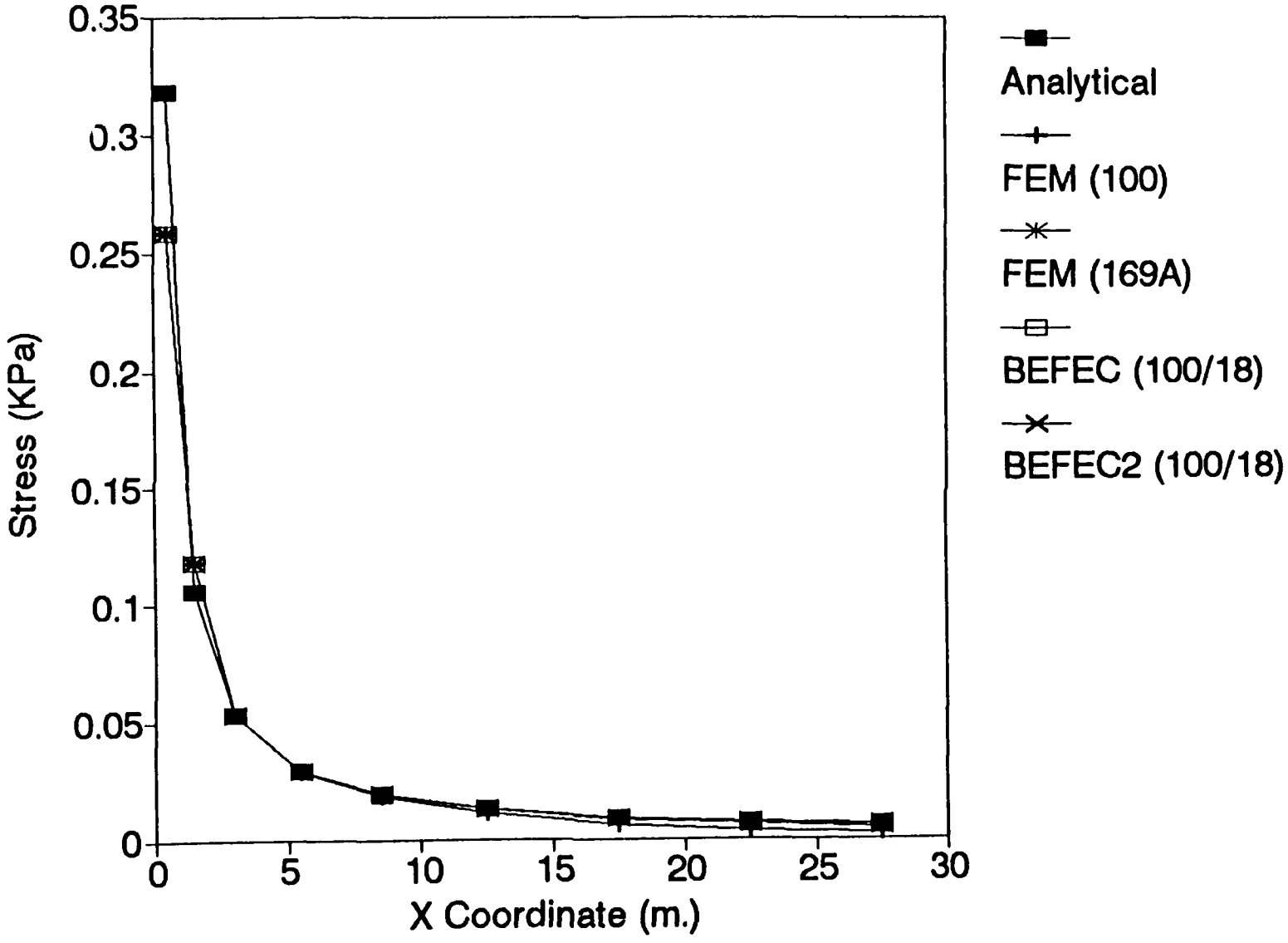

Fig. 10 Problem 1: Sigma-XY Along Diagonal Elements

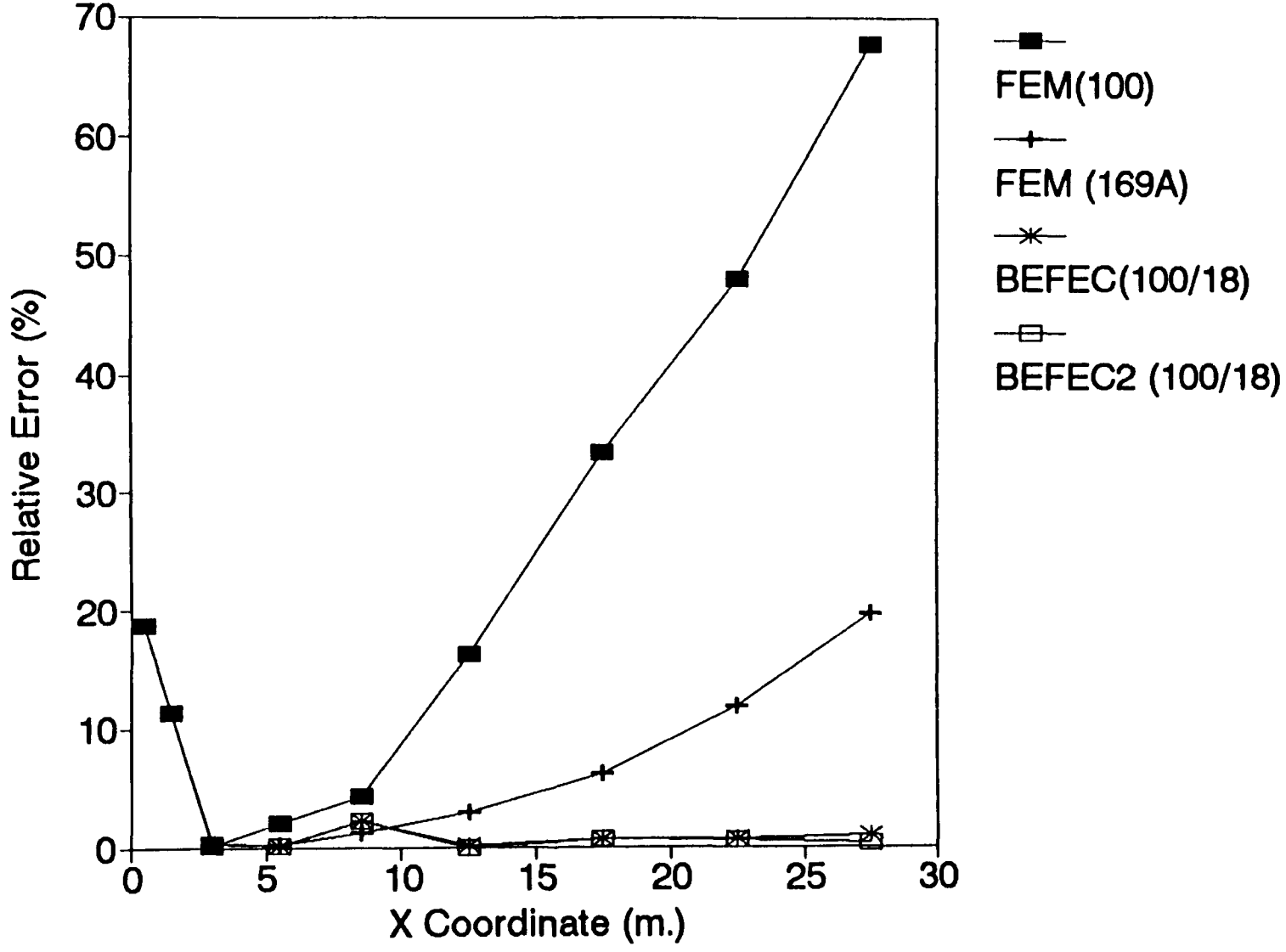

Fig. 11 Problem 1: Error in Sigma-XY Along Diagonal Elements

6. Vertical Normal Stresses (σ_{yy}) along the diagonal elements. Fig. (12) presents values of the computed stresses obtained from the respective analyses. It can be seen that near the region where the load is applied ($x < 2.5$ m.), all the solutions yield the similar values which over estimate the vertical stresses indicating effects of stress concentration are dominant within this region. It also indicates that the coupled boundary elements have no significant effect within this region. The relative error of the stresses are shown in fig. (13). From this graph we can see that the prediction of the stresses in the far field by the initial finite element analysis FEM (100) is in error by as much as 40%. This however is reduced to less that 4% when the mesh size is doubled FEM (169A). The coupled solution particularly the unsymmetric version BEFEC (100/18) results in a slightly better prediction as compared with FEM (169A) where stresses are within 2% of the analytical solution at the far field. It is only in this particular instance that there is a observable difference between the symmetric and unsymmetric coupling methods. The difference is significant enough such that the symmetric results are slightly less accurate than the those obtained using the expanded mesh.

Problem 2: Uniformly Distributed Load Applied to an Elastic Half-Plane. To solve this problem, five different analyses were considered namely: (1) a finite element analysis consisting of a 40 m. × 40 m. region using 121 nodes and 100 elements, FEM (121) [see fig. (14)], (2) a finite element analysis consisting of a 80 m. × 80 m. region using 225 nodes and 196 finite elements, FEM (225A) [see fig. (15)], (3) a finite element analysis consisting of a 40 m. × 40 m. region using 225 nodes and 196 finite elements FEM (225B), [see fig. (16)] and (4) a coupled boundary element/finite element analysis consisting of a 40 m. × 40 m. region with 121 nodes and 100 elements together with 20 boundary elements (BEFEC-121/20). (5) a coupled boundary element/finite element analysis similar to that performed in (4) but with the skew-symmetric part of the boundary element stiffness matrix discarded (BEFEC2-121/20). Symmetry in geometry was considered. The material properties were E=30 MPa, $\nu = 0.25$. The applied load had a magnitude of 1 KN/m and was applied over a length of 10 m.

Results were compared between the finite element solutions where the far field displacements were assumed to vanish and that using the boundary elements.

The following observations are made.

1. Vertical Displacements along the centerline: Because of symmetry along this line , the horizontal displacements are zero. Thus only vertical displacements were considered. The results are presented in fig (17). They show that using the conventional method of analysis, FEM (121), a significant disparity between the analytical and numerical solution. This discrepancy is affected very

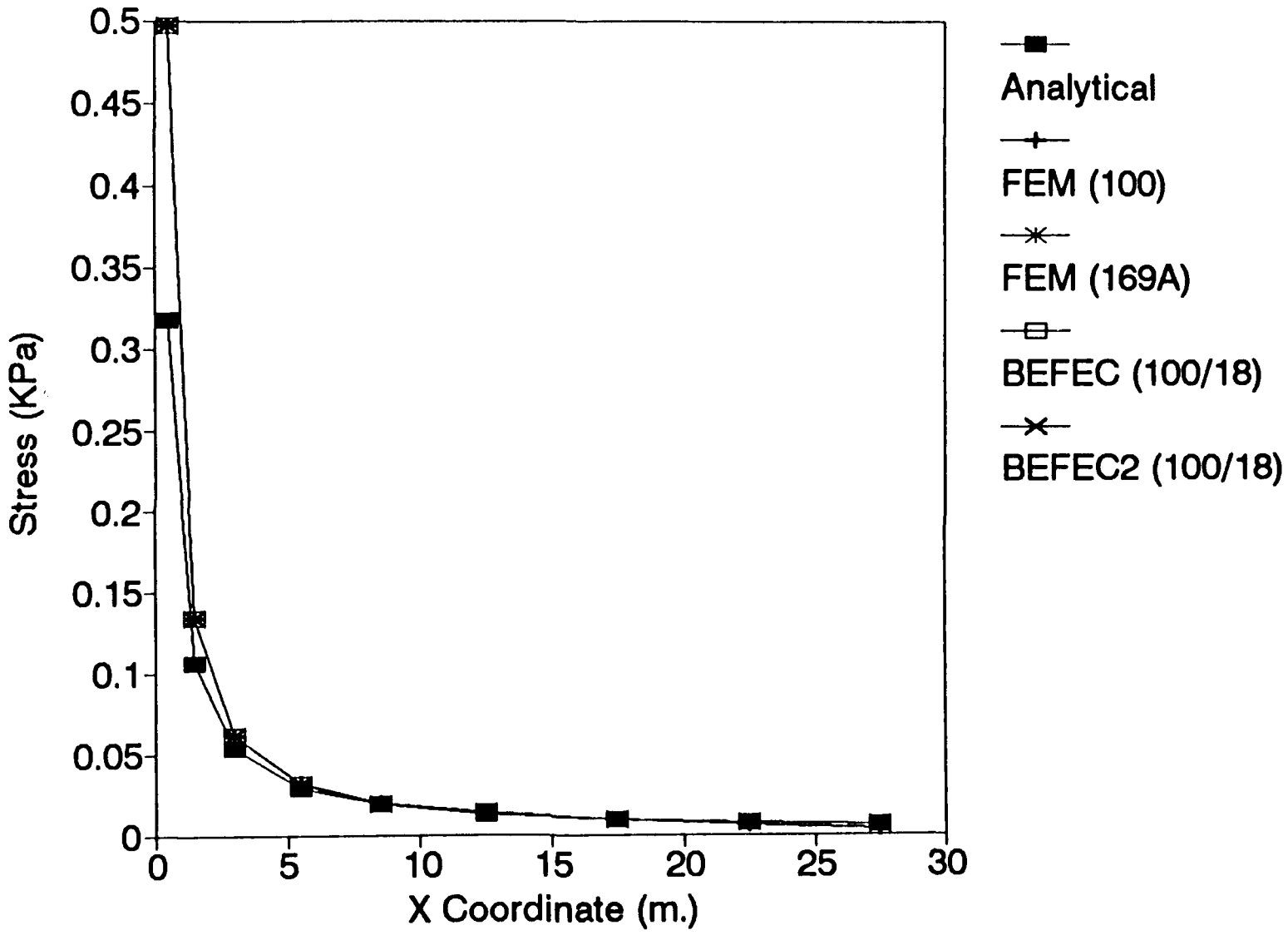

Fig. 12 Problem 1: Sigma-YY Along Diagonal Elements

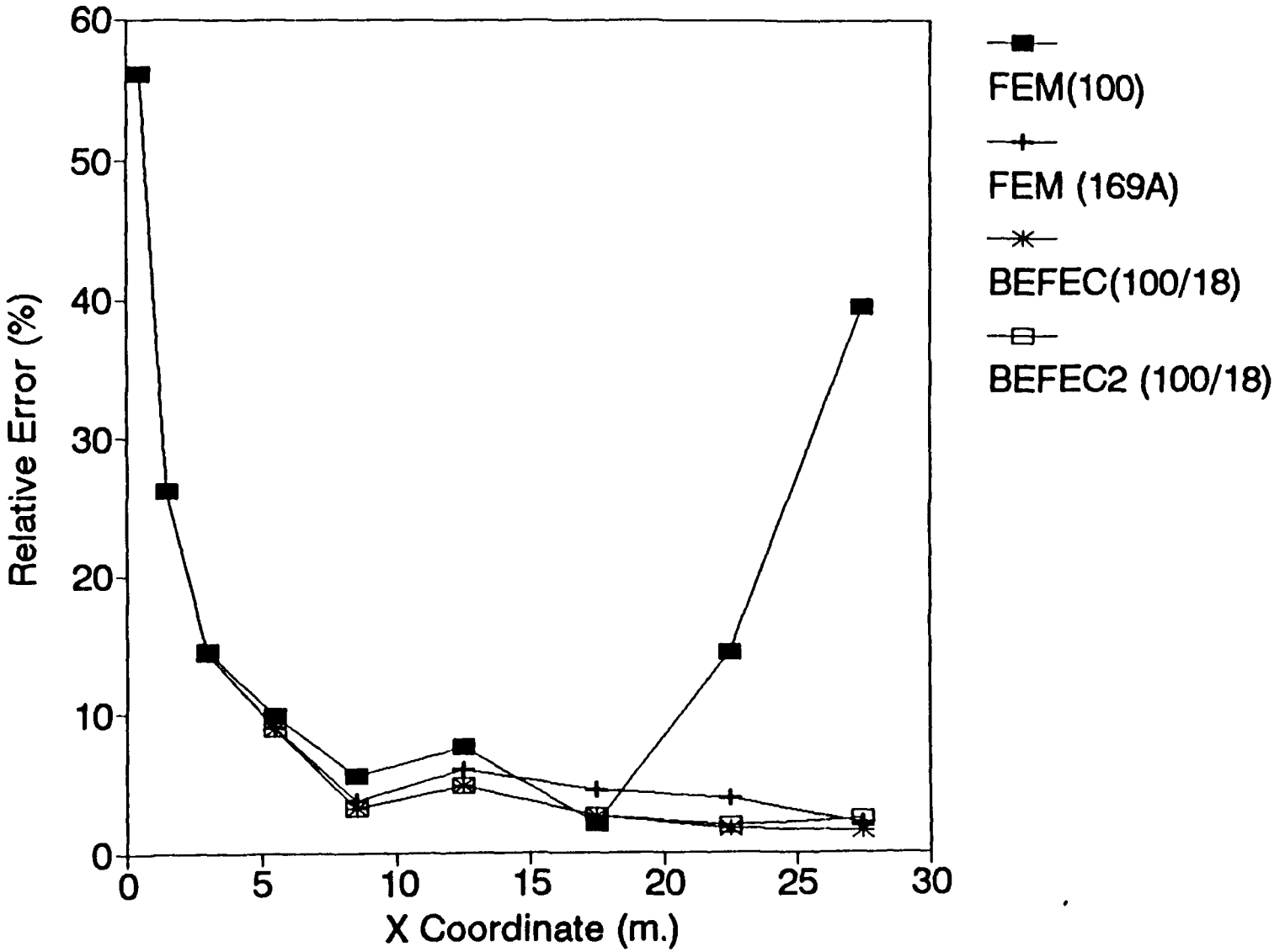

Fig. 13 Problem 1: Error in Sigma-YY Along Diagonal Elements

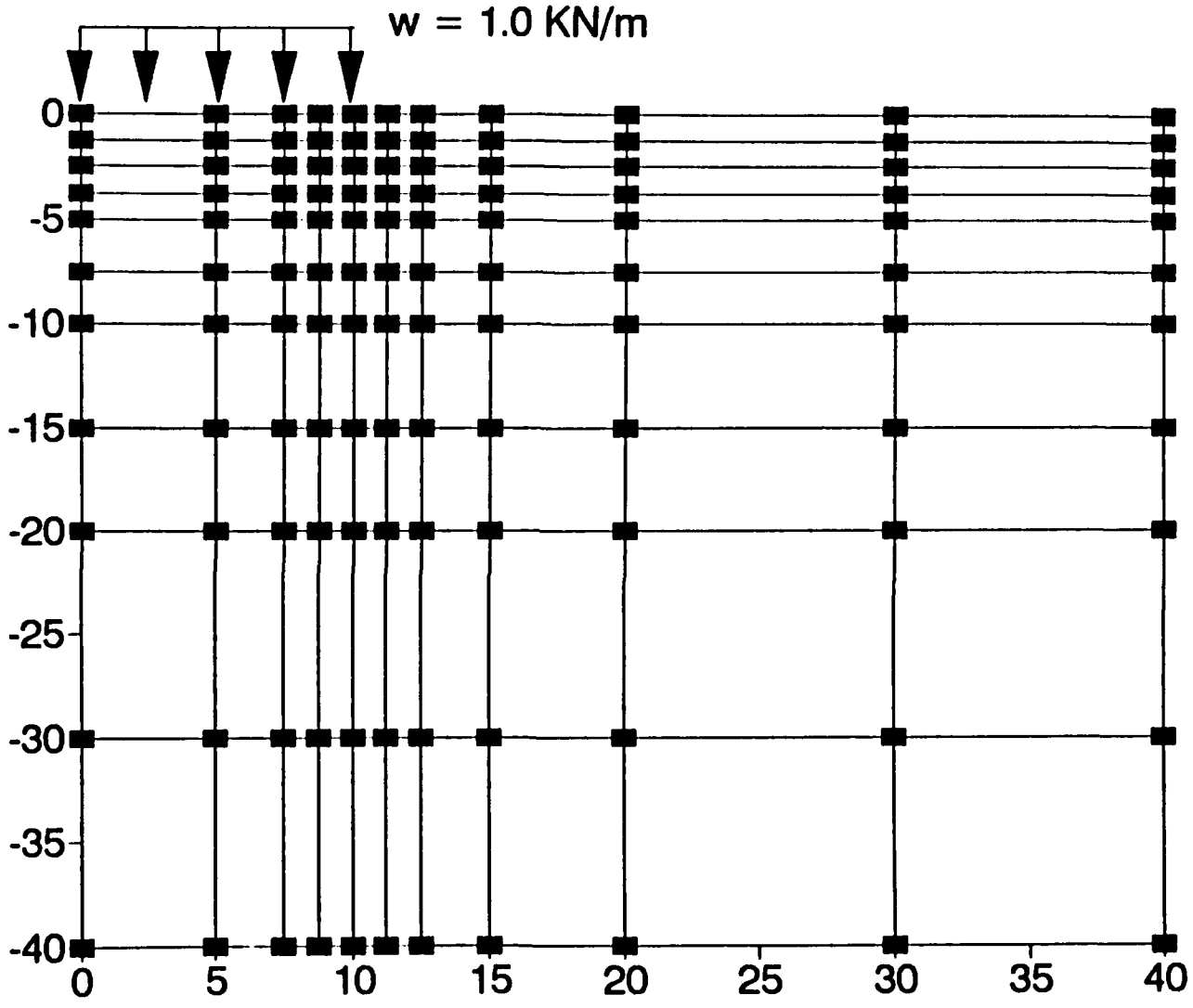

Fig. 14 FEM(121) Mesh

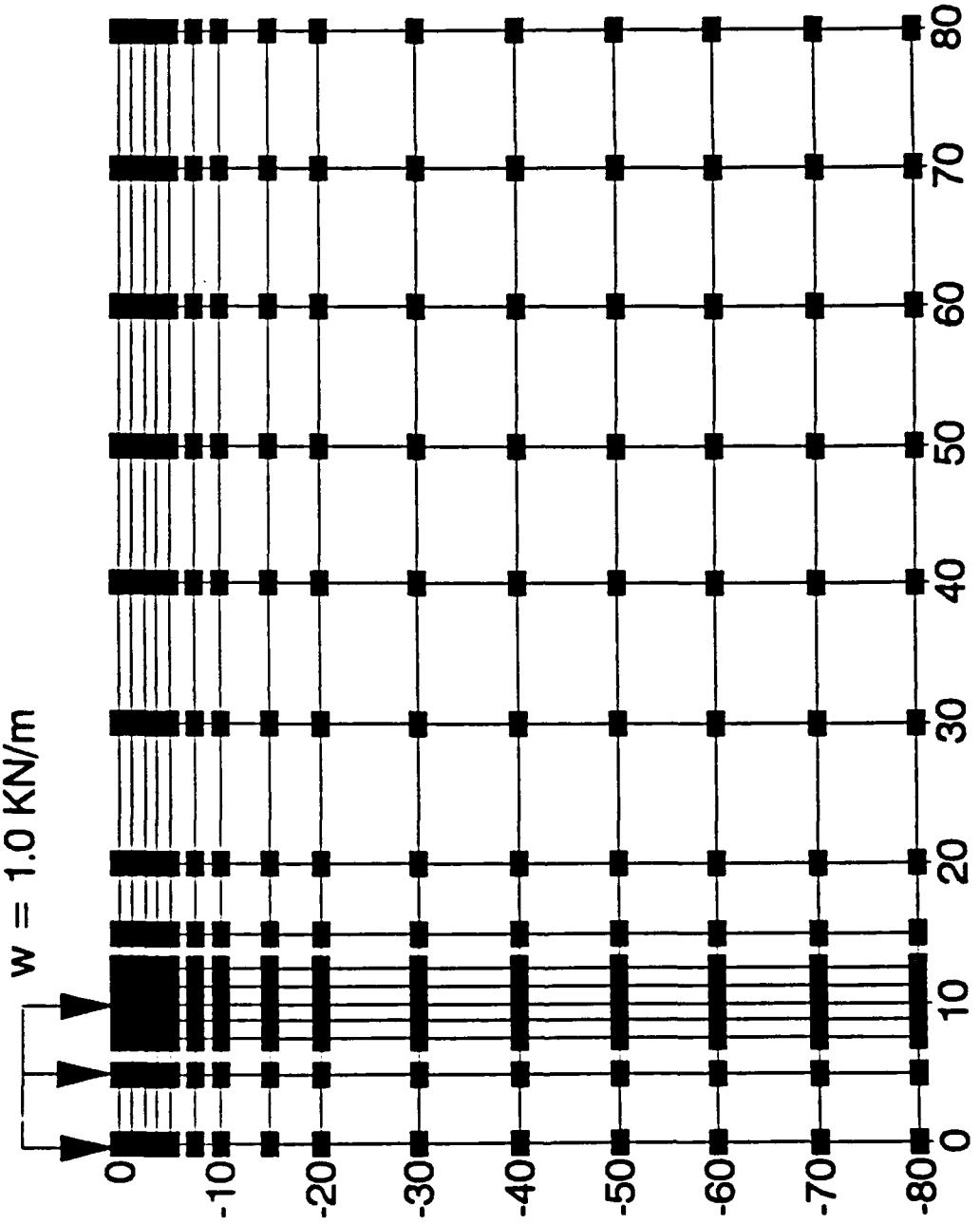

Fig. 15 FEM (225A) Mesh

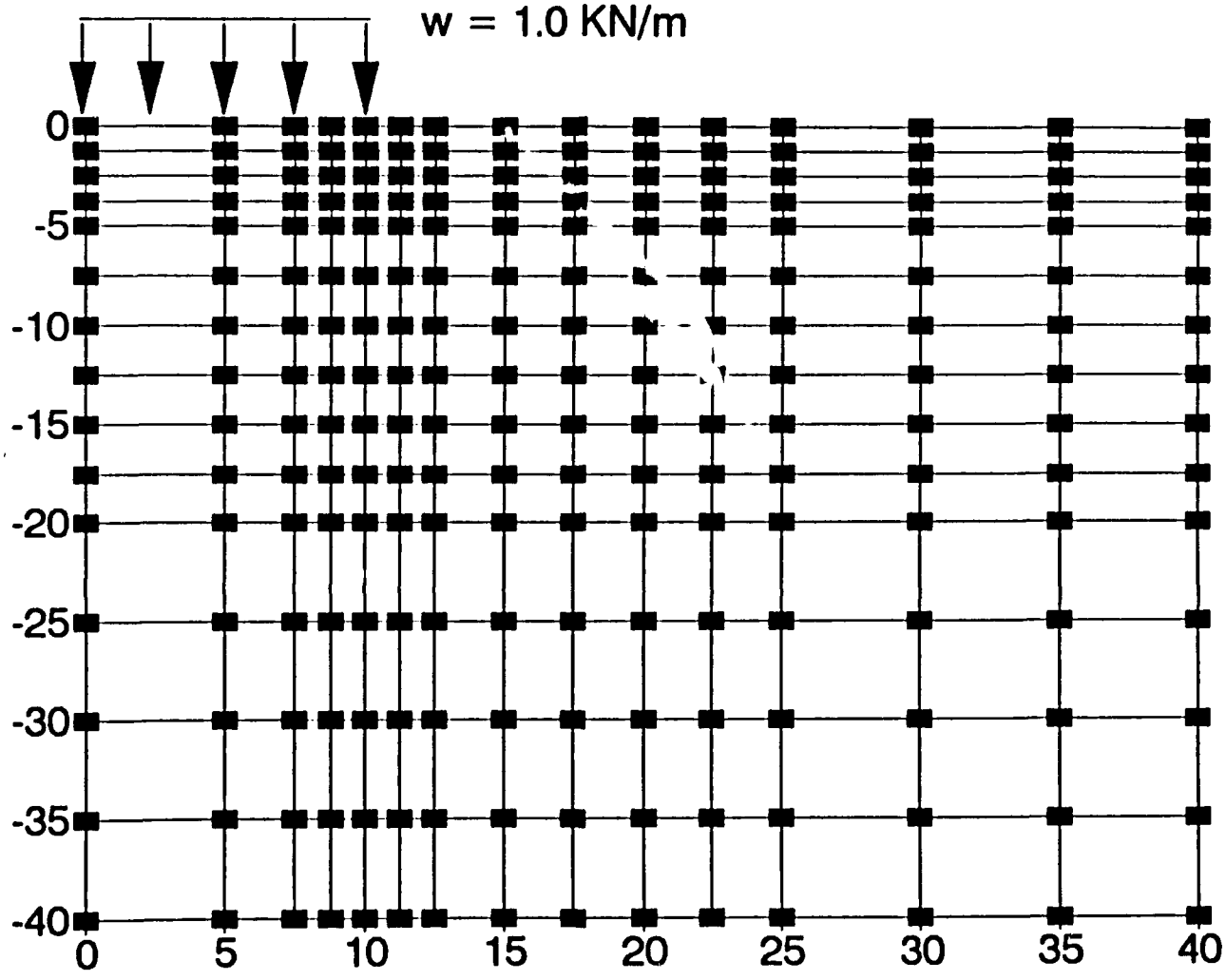

Fig. 16 FEM (225B) Mesh

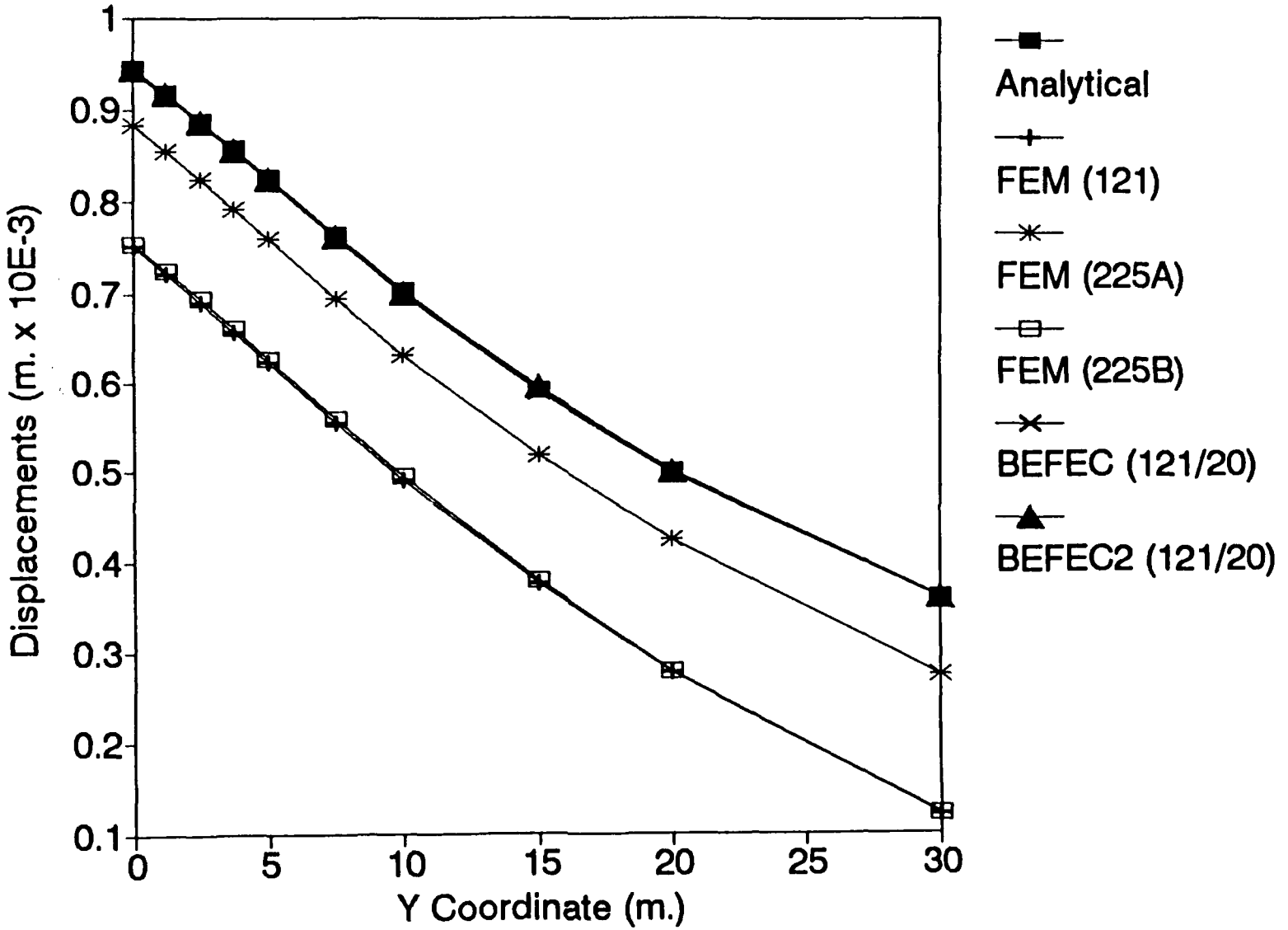

Fig. 17 Problem 2: Vertical Displacements Along Centerline

little by refining the mesh as was done in FEM (225B). The prediction of the vertical displacements along the centerline improved by coupling the solution with boundary element method BEFEC (121/20), BEFEC2 (121/20) or increasing the domain of the problem FEM (225A) the latter option giving a slightly better prediction the latter giving an answer very close to the analytical solution. As in the previous problem both symmetric and unsymmetric solutions give the same answer.

2. Horizontal displacements along the surface. Evaluating the analytical solution, it can be seen that the horizontal displacements along the traction free surface are a constant equal to

$$u_x\big|_{y=0} = \frac{-w(1-2\nu)}{2G} \qquad x > a$$

From fig. (18), it can be noted that in all five analyses, there is a substantial discrepancy between the numerical and analytical solution. Because in the finite element solutions, the horizontal displacements are assumed to vanish away from the loaded area, all three finite element solutions diverge from the analytical solution as points away from the loaded area are considered. Both of the coupled solutions give displacements which are close to the analytical solution due to the fact that the above property of the problem is modeled using the fundamental solution for the boundary element method. It should be stated however that increasing the domain of the problem results in an improvement of the predicted horizontal displacements.

3. Vertical displacements along the surface. Results presented in fig. (19) show that like the displacements along the centerline, the conventional method of finite element analysis FEM (121) results is a substantial disparity between the analytical and numerical solution. This disparity is little affected by refining the mesh as was done in FEM (225B). The prediction of vertical displacements can however be improved by coupling the solution with the boundary element method BEFEC (121/20), or increasing the domain of the problem as in FEM (225A). In this particular case, the displacements obtained using the coupled solution are much more accurate than the finite element solution.

4. Horizontal Normal Stresses (σ_{xx}) along the diagonal elements. From fig (20) it can be seen that the stresses predicted by the initial finite element method alone FEM (121) is slightly over predicted in the near field and considerably underpredicted in the far field. It is noteworthy to point out that increasing the domain as in FEM (225A) or coupling with the boundary element method BEFEC (121/20) increases that error in the overprediction of the stresses near the loaded area. These error can be attributed to the approximate representation of the distributed load with equivalent nodal loads. It should be pointed out that the greatest errors in this particular region results from the coupling of the finite element method with the boundary element method. In comparison, the coupled

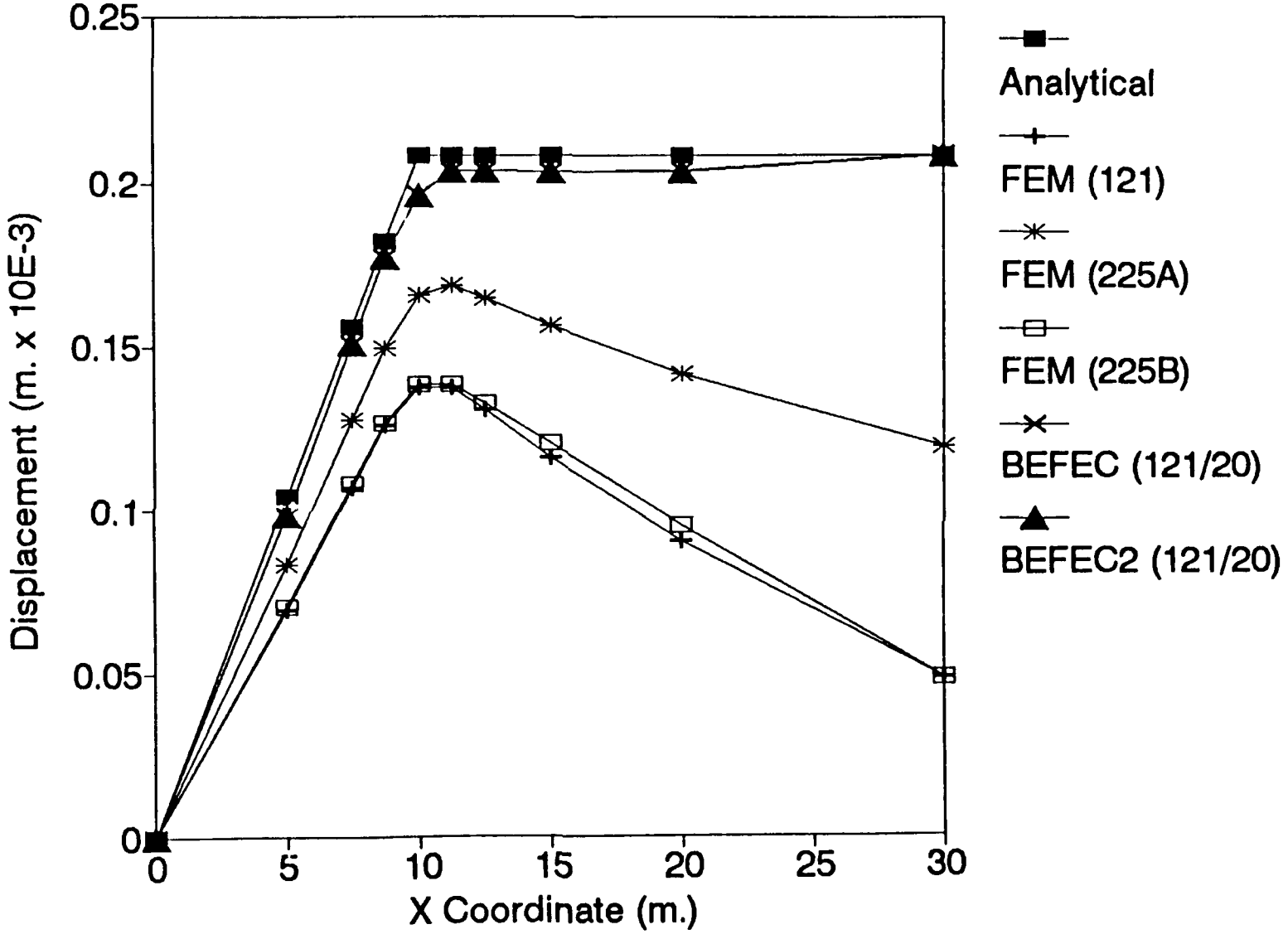

Fig. 18 Problem 2: Horizontal Displacements Along Surface

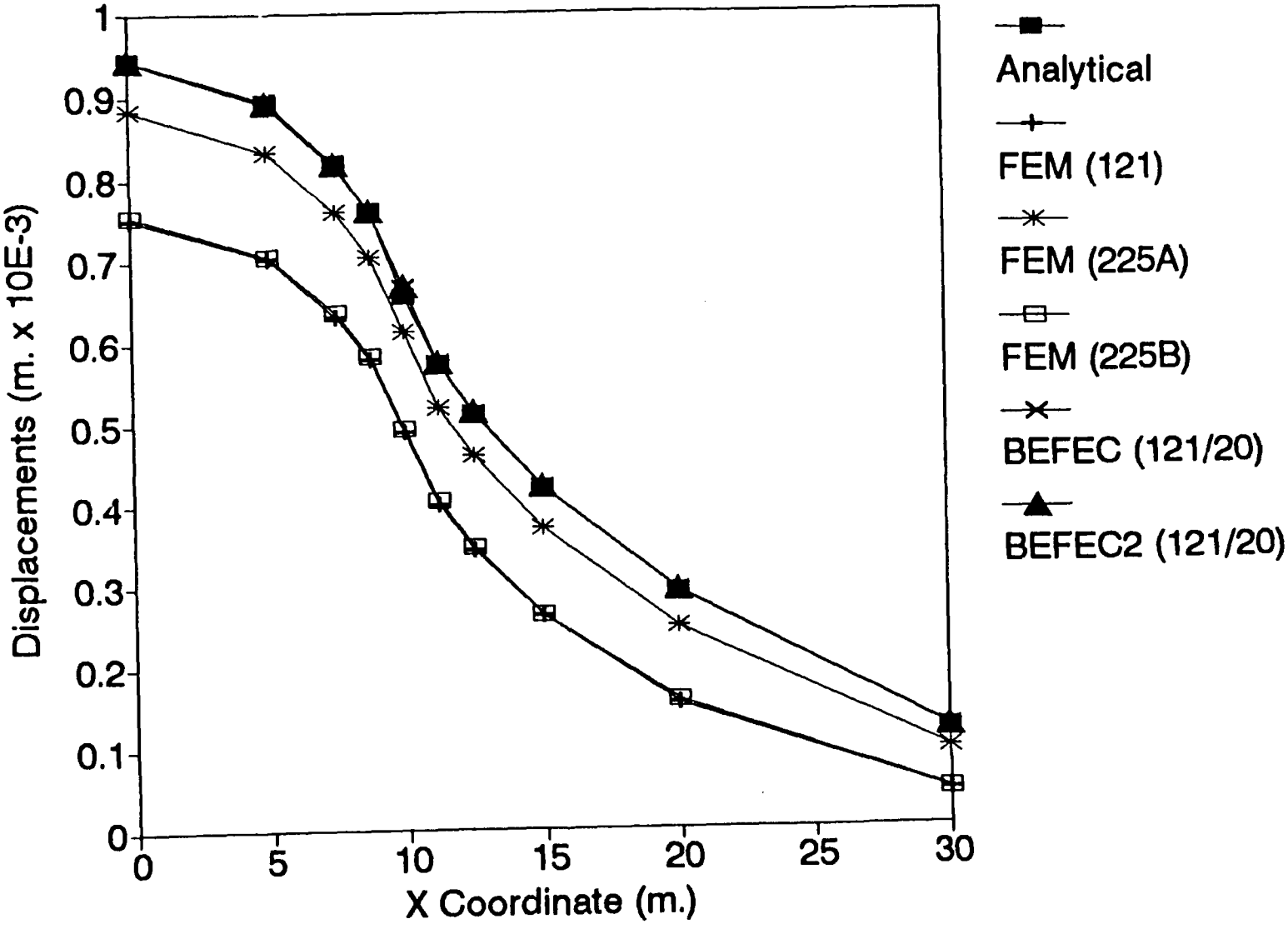

Fig. 19 Problem 2: Vertical Displacements Along Surface

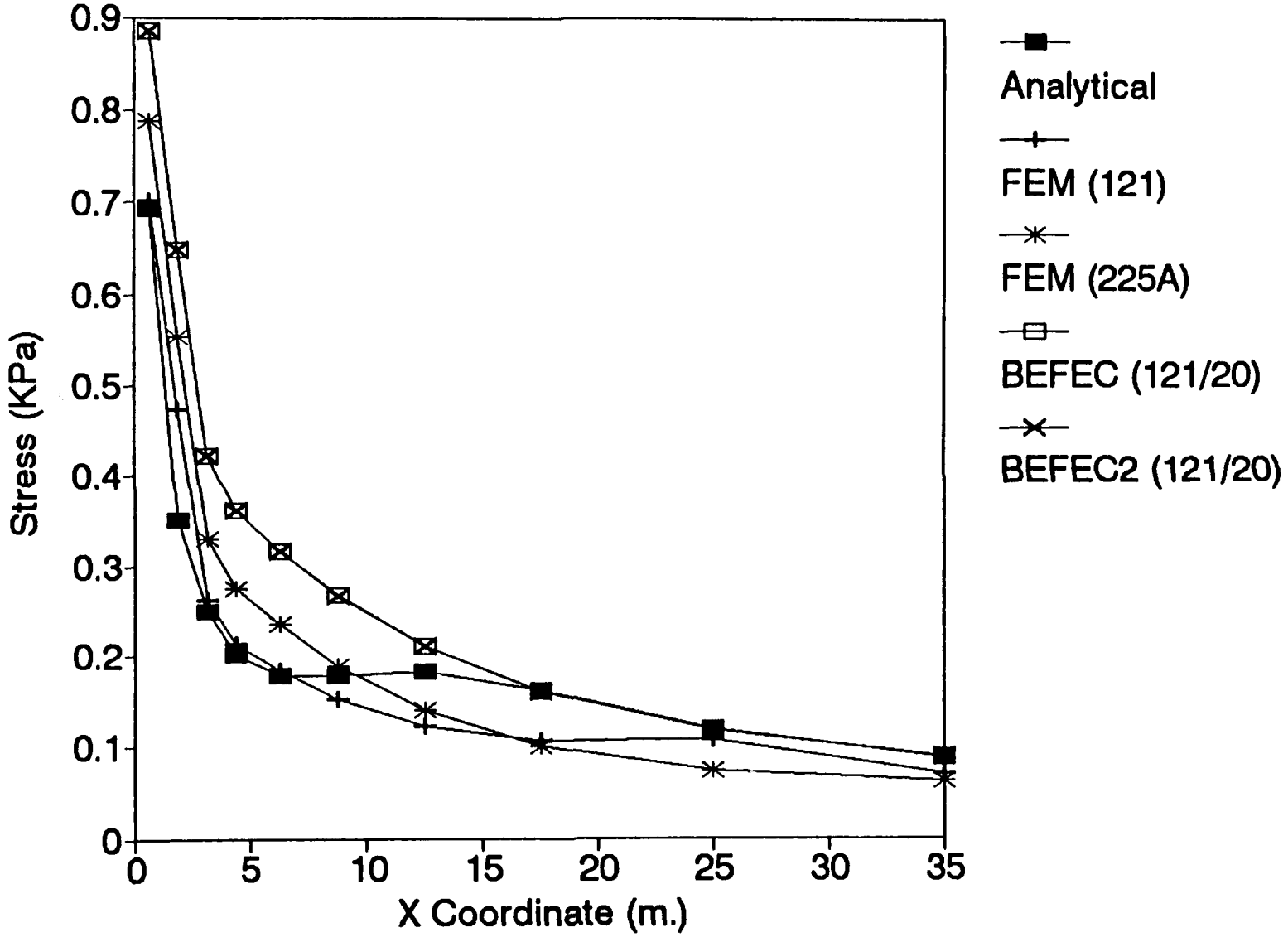

Fig. 20 Problem 2: Sigma-XX Along Diagonal Elements

method yielded stresses which agreed very will with the analytical solution in the far field. This is not true for the values obtained using the finite element method alone. Significant error were noted in the far field stresses. From the relative error of these stresses as shown in fig. (21) it can be seen that both analyses result in error of up to 40%. It should also be emphasized that expanding the finite element mesh as in FEM (225A) does not improve the prediction of stresses.

5. Shear Stresses (σ_{xy}) along the diagonal elements. Results of the analyses performed are presented in fig. (22). From the graph, it can be seen that there is a significant over prediction of the stresses in the region close to the loaded area. Also, it should be noted that all method resulted in similar predicted stresses. However, in the far field, the initial finite element solution FEM (121) significantly underpredicts the stresses. This underprediction is reduced by expanding the mesh as shown by FEM (255A). Results very close to the analytical solution are obtained when the solution is coupled with the boundary element method as in BEFEC (121/20) and BEFEC2 (121/20). Comparing the relative error as presented in fig. (23), it can be seen that the FEM (121) far field solution is grossly in error. In particular, an underprediction of 60% occurs in the initial finite element solution FEM (121). This error is substantially reduced to 20% by expanding the mesh to twice the initial size as in FEM (225A). The results obtained using both the unsymmetric BEFEC (121/20) and symmetric BEFEC2 (121/20) coupled solution yield identical values within 2% of the analytical solution.

6. Vertical Normal Stresses (σ_{yy}) along the diagonal elements. Fig. (24) presents values of the computed stresses obtained from the respective analyses. It can be seen from this graph that the effect of the approximation of the distributed load with equivalent nodal loads results in a significant underprediction of the stresses in all methods used. It can also be seen from this graph all methods examined yield similar values. The relative error of the stresses are shown in fig. (25). From this graph we can see that the prediction of the stresses in the far field by the initial finite element analysis FEM (121) is in error by as much as 30%. This however is reduced to less that 4% when the mesh size is doubled FEM (225A). The unsymmetric coupled solution BEFEC (121/20) results in a slightly better prediction as compared with FEM (225A) where stresses are within 3.5% of the analytical solution at the far field. It can also be seen that there is a significant difference in the symmetric and unsymmetric coupling technique with respect to the stresses computed in the far field. In the symmetric solution, the stresses in the far field were in error by as much as 5%. It can be concluded that in the prediction of the vertical normal stresses, expanding the mesh and symmetric coupling of the boundary element method result in similar results.

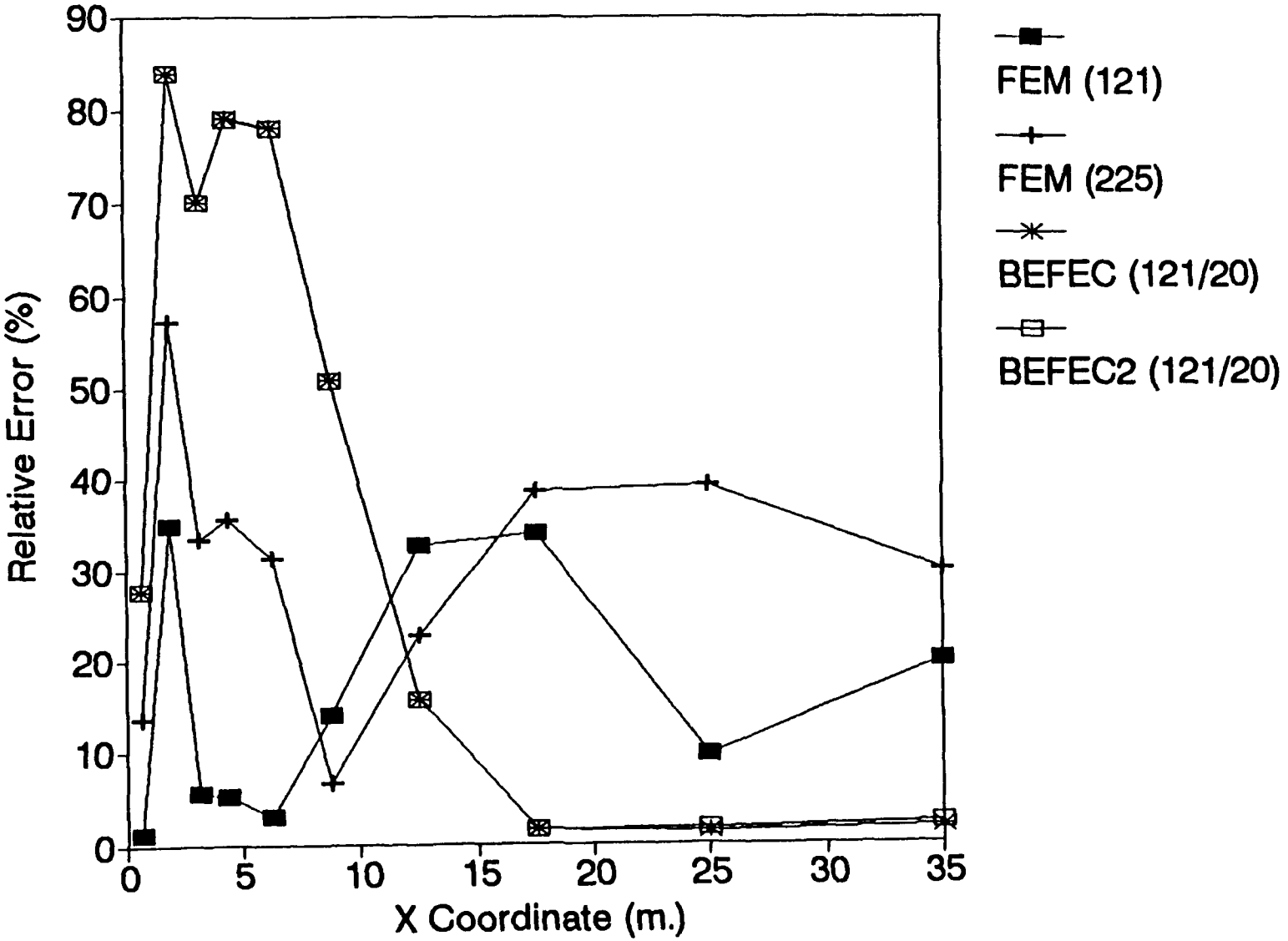

Fig. 21 Problem 2: Error in Sigma-XX Along Diagonal Elements

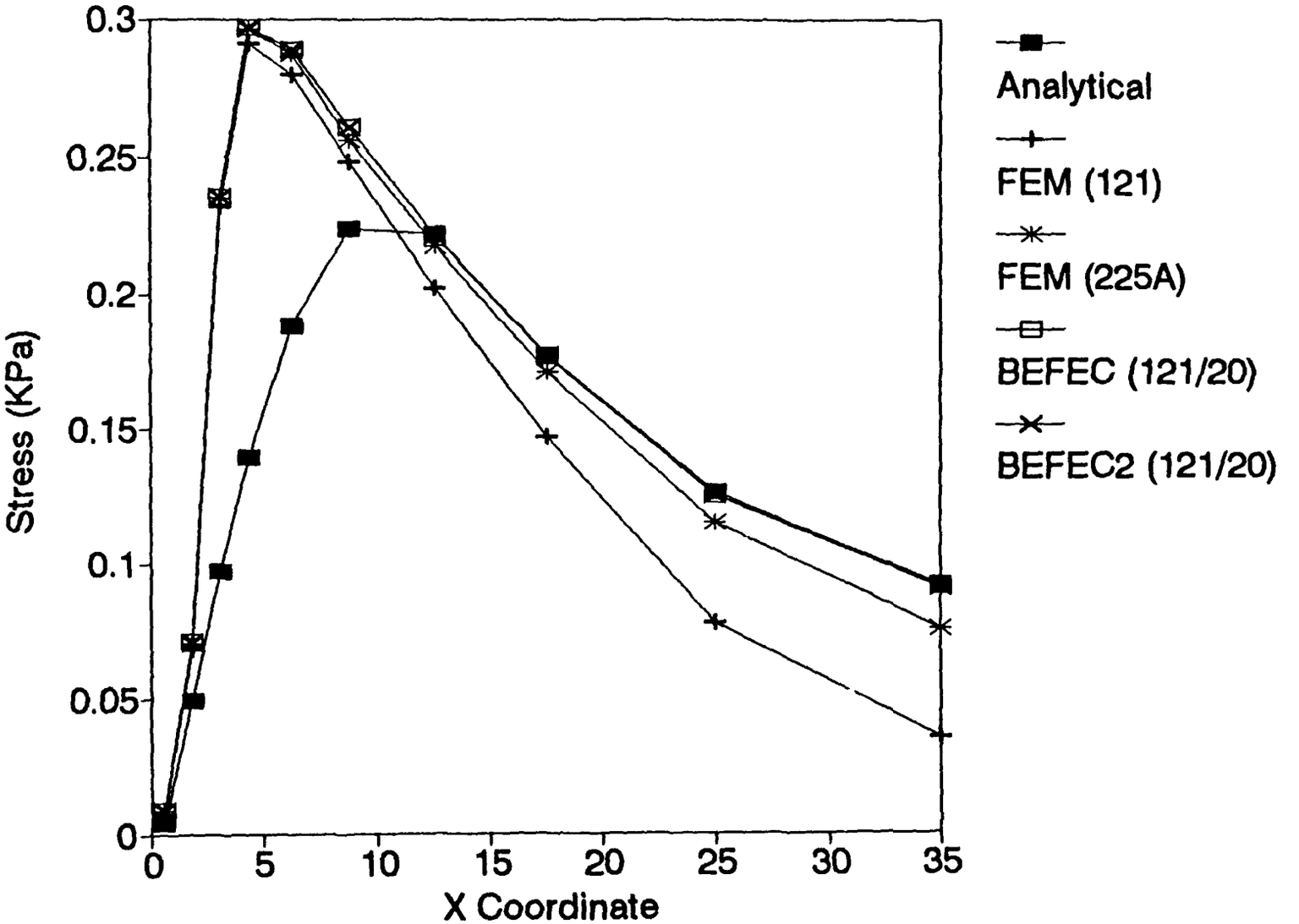

Fig. 22 Problem 2: Sigma-XY Along Diagonal Elements

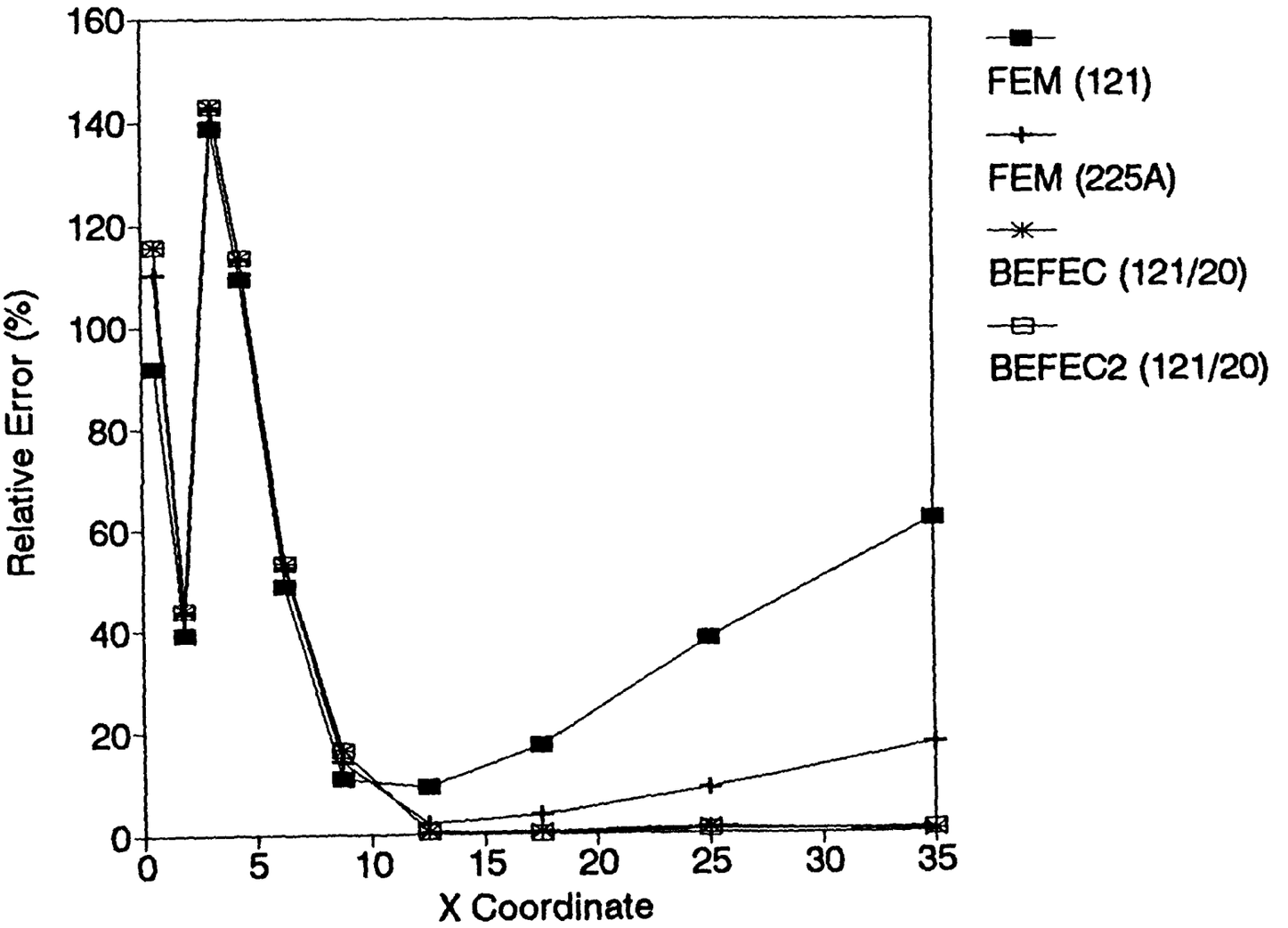

Fig. 23 Problem 2: Error in Sigma-XY Along Diagonal Elements

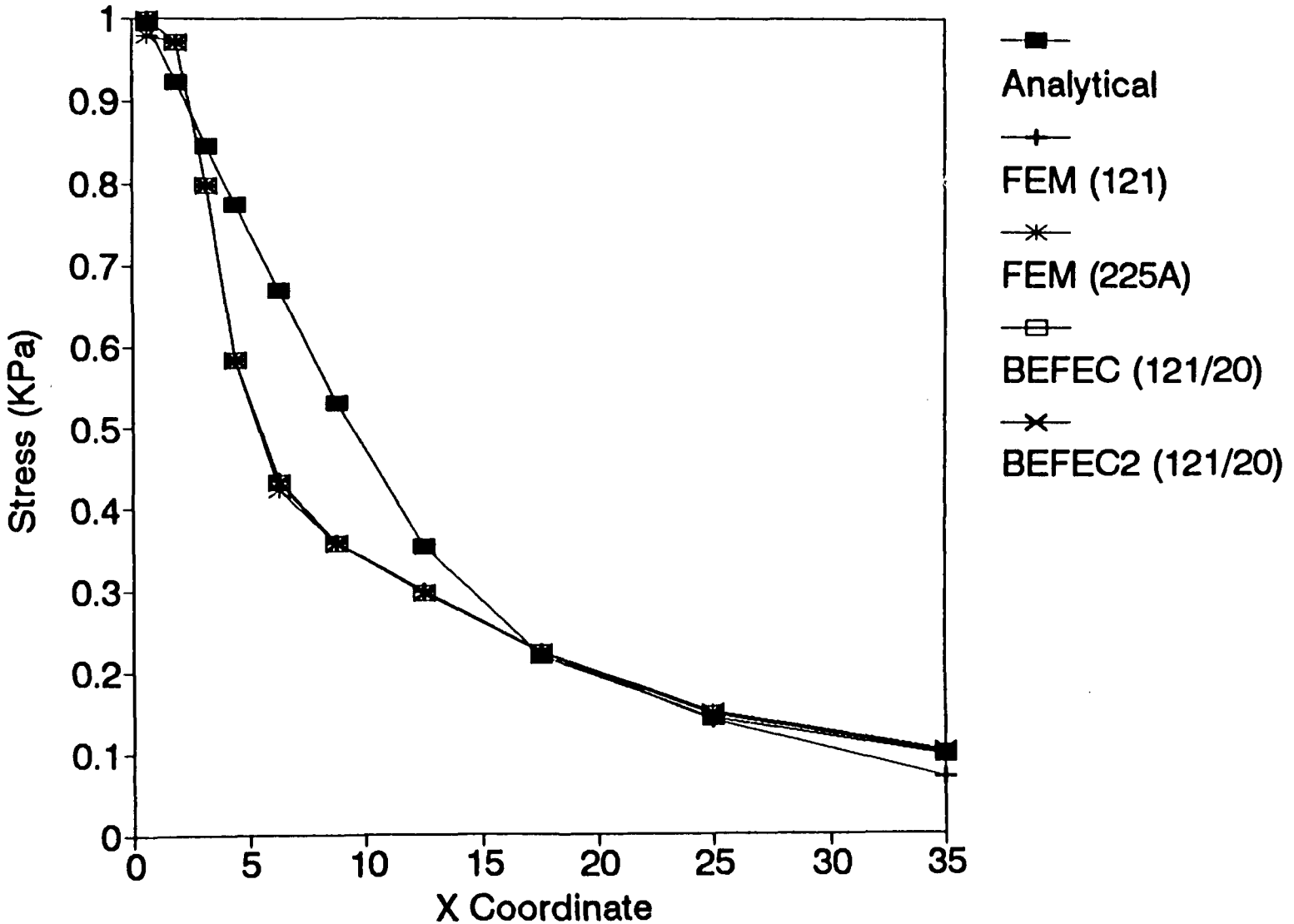

Fig. 24 Problem 2: Sigma-YY Along Diagonal Elements

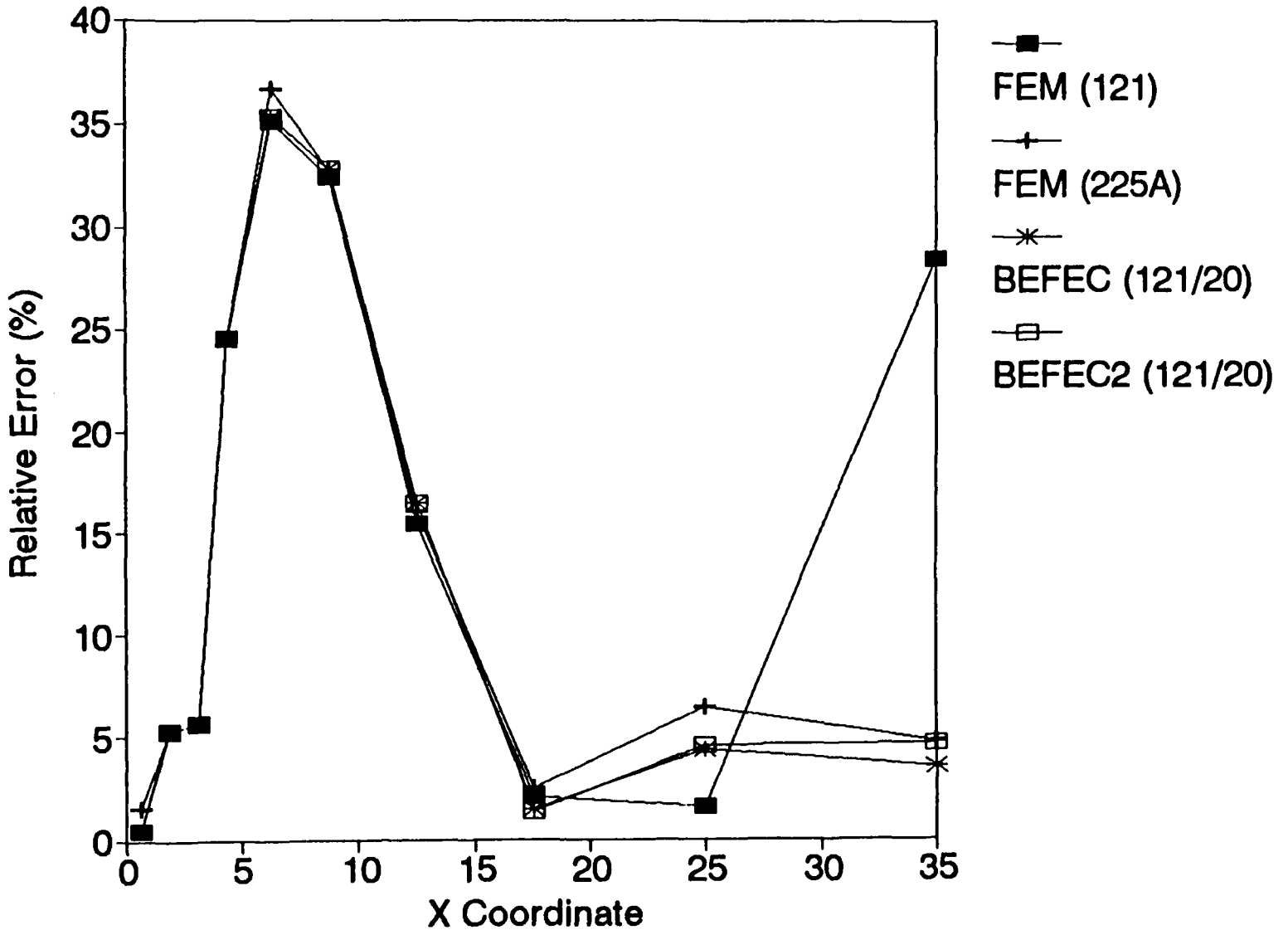

Fig. 25 Problem 2: Error in Sigma-YY Along Diagonal Elements

Conclusions and Recommendations

The following observations can be made with respect to the results of the proposed method of analysis.

1. The coupling of the boundary and finite element method provides an effective method for solving soil-structure interaction problems. The method has been shown to be efficient in solving linear problems involving infinite half-plane domains. Both the displacements and stresses obtained using this method are in close agreement with existing analytical solutions. It should be mentioned that the choice of the fundamental solution used in the boundary element method accounts for the efficiency of the method. This is because all degrees of freedom in the boundary element system are assembled in the finite element system. Thus the size of the boundary element system is kept to a minimum.

2. It was noted that for the problems solved, the difference between using the symmetric and unsymmetric part of the boundary element stiffness matrix is almost negligible with respect to the prediction of displacements. Thus it is possible to discard the skew-symmetric portion of the boundary element stiffness matrix and still obtain accurate answers.

3. Increasing the domain of the mesh does significantly reduce the error in the prediction of the far field vertical normal and shear stress but does not reduce the error in the prediction of the far field horizontal shear stress. In comparison, the use of the coupled method results in reduced error for all components of stress. Additionaly, these errors are significantly less than those resulting from the finite element method alone.

4. It should be emphasized that in the cases where identical results are obtained by expanding the finite element mesh and coupling the finite element method with the boundary element method, the latter approach is still more efficient because it results in far more less equations to be solved. It should also be pointed out that the results obtained by symmetric coupling are at worst as accurate as those obtained by expanding the mesh and at most times are as accurate as the unsymmetric coupling technique.

5. In the problem involving the concentrated load, it was observed that the stresses obtained using the finite element method was sufficiently accurate and the only significant errors occurred in the far field.

6. There is a significant discrepancy which results from the representation of the distributed load

with equivalent nodal loads. This discrepancy cannot be removed by either coupling the solution with the boundary element method or by modifying the mesh and these errors can even be intensified by using such methods.

REFERENCES

Brebbia, C. A. The Boundary Element Method for Engineers, Pentech Press Press, London, 1978.

Brebbia, C. A., J. C. F. Telles and L. C. Wrobel. Boundary Element Techniques: Theory and Applications in Engineering. Springer Verlag, Berlin, 1984.

Cristescu, M., G. Loubignac, Gaussian Quadrature Formulas for Functions with Singularities in 1/r Over Triangles and Quadrangles, in Recent Advances in Boundary Element Methods. Eds. C. A. Brebbia, 375-390, Pentech Press, London, 1978 .

Crouch, Steven L., A. M. Starfield, Boundary Element Methods in Solid Mechanics. George Allen and Unwin, 1983.

Georgiou, P. The Coupling of the Direct Boundary Element Method with the Finite Element Displacement Technique in Elastostatics. Ph.D. Dissertation, Southhampton University, 1981

Hughes, T., The Finite Element Method: Linear Static and Dynamic Finite Element Analysis Prentice Hall, Inc., Englewood Cliffs, New Jersey, 1987.

Manolis, G. D., D. E. Beskos, Boundary Elements in Elastodynamics, Allen and Unwin, Winchester, 1988.

Melan, E., Der Spannungszustand der durch eine Einselkraft im Innern beanspruchten Halbscheibe. Z. Angew. Math. Mech., 12 : 343-346, (1932)

Telles, Jose F. C., C. A. Brebbia, BoundaryElement Solution for Half-Plane Problems, Int. Journal of Solids and Structures 17, 1149-1158, 1981

Wolf, John P., Soil-Structure Interaction Analysis in the Time Domain, Prentice Hall, Englewood Cliffs, New Jersey, 1988.

Vallabhan, C. V. Girija, J. Sivakumar, N. Radhakrishnam, Application of Boundary Element Methods for Soil-Structure Interaction Problems. Proc. 6th Int. Conf. BEM (Boundary Elements), 6:27-39, Springer Verlag, 1986.

Zeng, Zhao-Jing and Rui-Ying Cai, Treatment of Singular Intgeral Caused by Employing Linear Boundary Elements for Two-Dimensional Elastostatic Problems. Computers and Structures, Vol. 34, No. 6, pp. 855-859, Pergamon Press, New York, 1990.

APPENDIX A

Analytical Solutions to Example Problems

In this appendix, the complete analytical solution to the problems solved are presented. These consist of: (1) A vertical concentrated load applied to the surface of an elastic half-space, (2) A distributed load applied to the surface of an elastic half-plane.

A.1 Concentrated Load Applied to an Elastic Half-Plane

The displacements and stresses corresponding to this problem are given by

$$u_x = \frac{P_y}{2\pi G}\left[(1-2\nu)\left(\arctan\frac{y}{x}+\frac{\pi}{2}\right)+\frac{xy}{x^2+y^2}\right]$$

$$u_y = \frac{P_y}{2\pi G}\left[-2(1-2\nu)\ln\left(\frac{x^2+y^2}{L^2}\right)^{1/2}+\frac{y^2}{x^2+y^2}\right]$$

$$\sigma_{xx} = -\frac{2P_y}{2}\frac{x^2y}{r^4} \qquad \sigma_{xx} = -\frac{2P_y}{2}\frac{x^2y}{r^4} \qquad \sigma_{xx} = -\frac{2P_y}{2}\frac{x^2y}{r^4}$$

where the load P_y is applied at the origin, while the displacements and stresses are evaluated at the point (x,y) and r is the distance from the origin to the point (x,y) such that $r = \sqrt{x^2+y^2}$. The constant G is the shear modulus, ν is poisson's ratio and L is an arbitrary constant chosen so that at the point $(L,0)$, $u_y = 0$.

A.2 Distributed Load Applied to the Surface of an Elastic Half-Plane

The displacements and stresses corresponding to this problem are given by

$$u_x = \frac{-w}{2\pi G}\left[(1-2\nu)\{(x-a)\,\theta_1-(x+a)\,\theta_2-\pi a)\}+(1-\nu)\,y\,\ln(r_1^2/r_2^2)\right]$$

$$u_y = \frac{-w}{2\pi G}\left[-(1-2\nu)\,y\,(\theta_1-\theta_2)+(1-\nu)\{(x-a)\ln(r_1^2)-(x+a)\ln(r_2^2)\right.$$

$$\left.+(L+a)\ln(L+a)^2-(L-a)\ln(L-a)^2\}\right]$$

$$\sigma_{xx} = \frac{-w}{\pi}\left[\theta_1 - \theta_2 + y(x-a)/r_1^2 - y(x+a)/r_2^2\right]$$

$$\sigma_{yy} = \frac{-w}{\pi}\left[\theta_1 - \theta_2 - y(x-a)/r_1^2 + y(x+a)/r_2^2\right]$$

$$\sigma_{xy} = \frac{-wy}{\pi}\left[1/r_1^2 - 1/r_2^2\right]$$

In these expressions, the following abbreviations are used

$$\theta_1 = \arctan\frac{y}{x-a} \qquad \theta_2 = \arctan\frac{y}{x+a}$$

$$r_1^2 = (x-a)^2 + y^2 \qquad r_2^2 = (x+a)^2 + y^2$$

where the distributed load w is applied from points $(-a,0)$ to $(a,0)$, while the displacements and stresses are evaluated at the point (x,y) and r is the distance from the origin to the point (x,y) such that $r = \sqrt{x^2+y^2}$. The constant G is the shear modulus, ν is poisson's ratio and L is an arbitrary constant chosen so that at the point $(L,0)$, $u_y = 0$.

APPENDIX B

Fundamental Solution

In this appendix the fundamental solution for the displacements and stresses due to a unit load applied to a half-plane is presented. The complete solution consists of two parts namely: (1) the Kelvin solution representing the solution to an infinite plane, (2) the complementary solution which when added to the Kelvin solution gives the half-plane solution. Thus the complete solution can be written as follows:

$$u^*_{ij} = u^k_{ij} + u^c_{ij} \tag{B.1}$$

$$\sigma^*_{ijk} = \sigma^k_{ijk} + \sigma^c_{ijk} \tag{B.2}$$

where u^*_{ij} is the displacement in the i direction due to a unit load in the j direction and σ^*_{ijk} is ijth component of stress due to a unit load in the k direction. The geometry of the problem is given in figure B1.

B.1 Kelvin Solution

$$u^k_{11} = \frac{1}{8\pi G(1-\nu)}\left[(3-4\nu)\ln\left(\frac{1}{r}\right) + \frac{x^2}{r^2}\right]$$

$$u^k_{12} = \frac{1}{8\pi G(1-\nu)}\left[\frac{xy}{r^2}\right]$$

$$u^k_{21} = \frac{1}{8\pi G(1-\nu)}\left[\frac{xy}{r^2}\right]$$

$$u^k_{22} = \frac{1}{8\pi G(1-\nu)}\left[(3-4\nu)\ln\left(\frac{1}{r}\right) + \frac{y^2}{r^2}\right]$$

$$\sigma^k_{111} = \frac{1}{4\pi(1-\nu)r}\left\{(1-2\nu)\left(\frac{x}{r}\right) + \frac{x^3}{r^3}\right\}$$

$$\sigma^k_{121} = \frac{1}{4\pi(1-\nu)r}\left\{(1-2\nu)\left(\frac{y}{r}\right) + \frac{x^2 y}{r^3}\right\}$$

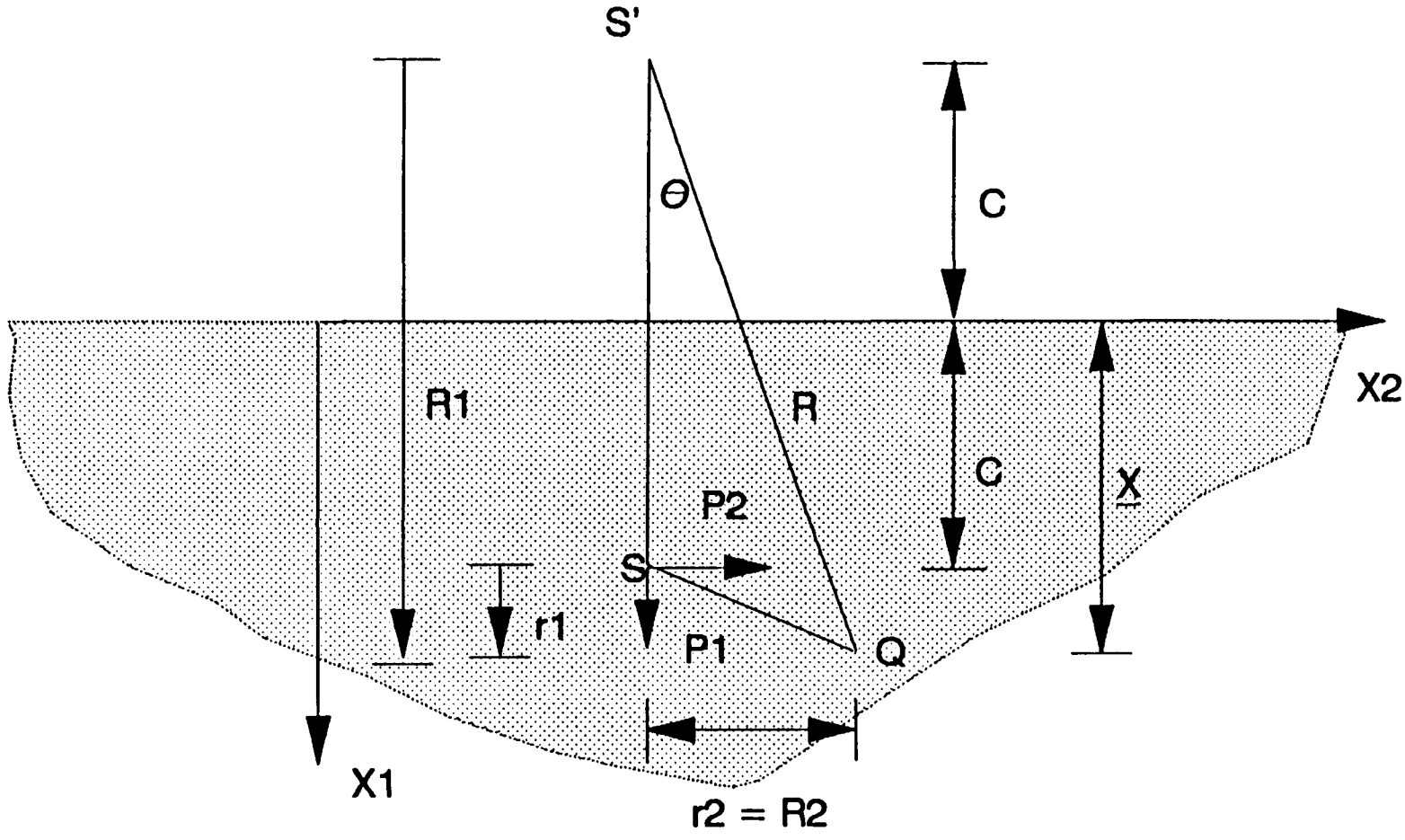

Figure B.1 Unit Load Applied to an Elastic Half-Plane

$$\sigma^k_{221} = \frac{1}{4\pi(1-\nu)r}\left\{(1-2\nu)(\frac{x}{r}) + \frac{xy^2}{r^3}\right\}$$

$$\sigma^k_{112} = \frac{1}{4\pi(1-\nu)r}\left\{(1-2\nu)(\frac{y}{r}) + \frac{x^2y}{r^3}\right\}$$

$$\sigma^k_{122} = \frac{1}{4\pi(1-\nu)r}\left\{(1-2\nu)(\frac{x}{r}) + \frac{xy^2}{r^3}\right\}$$

$$\sigma^k_{222} = \frac{1}{4\pi(1-\nu)r}\left\{(1-2\nu)(\frac{y}{r}) + \frac{y^3}{r^3}\right\}$$

B.2 Complementary Solution

$$u^c_{11} = K_d\left\{-[8(1-\nu)^2 - (3-4\nu)]\, ln\, R + \frac{[(3-4\nu)R_1^2 - 2x\,\hat{x}]}{R^2} + \frac{4x\,\hat{x}\,R_1^2}{R^4}\right\}$$

$$u^c_{12} = K_d\left\{\frac{(3-4\nu)r_1r_2}{R^2} + \frac{4x\,\hat{x}\,R_1r_2}{R^4} - 4(1-\nu)(1-2\nu)\theta\right\}$$

$$u^c_{21} = K_d\left\{\frac{(3-4\nu)r_1r_2}{R^2} - \frac{4x\,\hat{x}\,R_1r_2}{R^4} + 4(1-\nu)(1-2\nu)\theta\right\}$$

$$u^c_{22} = K_d\left\{-[8(1-\nu)^2 - (3-4\nu)]\, ln\, R + \frac{[(3-4\nu)r_2^2 - 2x\,\hat{x}]}{R^2} + \frac{4x\,\hat{x}\,r_2^2}{R^4}\right\}$$

$$\sigma^c_{111} = -K_s\left\{\frac{(3\hat{x}+x)(1-2\nu)}{R^2} + \frac{2R_1(R_1^2 + 2x\,\hat{x}) - (4\hat{x}r_2^2)(1-2\nu)}{R^4} - \frac{16x\,\hat{x}\,R_1r_2^2}{R^6}\right\}$$

$$\sigma^c_{121} = -K_s r_2 \left\{ -\frac{(1-2\nu)}{R^2} + \frac{2[\, x^2 - 2x\hat{x} - \hat{x}^2 + 2xR_1(1-2\nu)]}{R^4} + \frac{16x\,\hat{x}\,R_1^2}{R^6} \right\}$$

$$\sigma^c_{221} = -K_s \left\{ \frac{(x+3\hat{x})(1-2\nu)}{R^2} + \frac{2[\, R_1(r_2^2+2\hat{x}^2) - 2\hat{x}r_2^2 + 2xr_2^2(1-2\nu)]}{R^4} + \frac{16x\,\hat{x}\,R_1^2}{R^6} \right\}$$

$$\sigma^c_{112} = -K_s r_2 \left\{ \frac{(1-2\nu)}{R^2} - \frac{2[\, \hat{x}^2 - x^2 + 6x\hat{x} - 2xR_1(1-2\nu)]}{R^4} + \frac{16x\,\hat{x}\,r_2^2}{R^6} \right\}$$

$$\sigma^c_{122} = -K_s \left\{ \frac{(3\hat{x}+x)(1-2\nu)}{R^2} + \frac{2[(2x\,\hat{x}+r_2^2)R_1 - 2xR_1^2(1-2\nu)]}{R^4} - \frac{16x\,\hat{x}\,R_1 r_2^2}{R^6} \right\}$$

$$\sigma^c_{222} = -K_s r_2 \left\{ \frac{3(1-2\nu)}{R^2} - \frac{2[\, r_2^2 - 4x\hat{x} - 2\hat{x}^2 - 2xR_1(1-2\nu)]}{R^4} + \frac{16x\,\hat{x}\,R_1^2}{R^6} \right\}$$

where

$$\theta = arctan\left(\frac{r_2}{R_1}\right)$$

$$K_d = \frac{1}{[8\pi(1-\nu)G]}$$

$$K_s = \frac{1}{[4\pi(1-\nu)]}$$

APPENDIX C

Derivation of Transformation Matrix

From the finite element method, the equivalent nodal loads f_{ij} for a given traction distribution $h(\xi,\eta)$ over the boundary Γ are given by

$$f_{ij} = \int_{\Gamma} h_i(\xi,\eta)\psi_j(\xi,\eta)\ d\Gamma \tag{C.1}$$

where $h_i(\xi,\eta)$ is the ith traction compoenent, $\psi_j(\xi,\eta)$ is the lagrangian interpolating functions corresponding to the jth node. Because of the properties of the interpolating function, only to those components corresponding to nodes on the boundary Γ are non-zero. Furthermore, these non-vanishing components degenerate to functions in one variable. Thus, the above integral can be rewritten as

$$f_{ij} = \int_{\Gamma} h_i(\zeta)\psi_j(\zeta)\ d\Gamma \tag{C.2}$$

where ζ is the coordinate along the boundary Γ.

Similarly, from the boundary element method it is assumed that the tractions over the entire element vary in the following manner

$$h_i(\zeta) = h_{ij}\psi_j(\zeta) \tag{C.3}$$

where h_{ij} is the ith component of the traction at the jth node.

Thus, combining the two above equations, the equivalent nodal loads can be obtained by the ation

$$f_{ij} = h_{ik}N_{kj} \tag{C.4}$$

where

$$N_{kj} = \int_{\Gamma} \psi_k(\zeta)\ \psi_j(\zeta)\ d\zeta \tag{C.5}$$

For the coupling between a bilinear quadrilateral finite element and linear boundary element, the corresponding shape functions are given by

$$\psi_1(\zeta) = \tfrac{1}{2}(1-\zeta) \qquad \psi_2(\zeta) = \tfrac{1}{2}(1+\zeta) \tag{C.6}$$

If the boundary Γ is a straight line of length l, the integral in the above equal evaluates to

$$N_{ij} = \frac{l}{6}\begin{bmatrix} 2 & 1 \\ 1 & 2 \end{bmatrix} \tag{C.7}$$

For a general boundary element system, the above matrix must be assembled into the global N matrix very similar to the way line elements are assembled in a finite element system.

Waterways Experiment Station Cataloging-In-Publication Data

Kuppusamy, T.

Solution of soil-structure interaction problems by coupled boundary element-finite element method / by T. Kuppusamy, Mark A. Zarco and Robert M. Ebeling ; prepared for Department of the Army, U.S. Army Corps of Engineers.

57 p. : ill. ; 28 cm. — (Technical report ; ITL-92-3)

Includes bibliographic references.

1. Soil-structure interaction — Mathematics. 2. Finite element method. 3. Boundary element methods. I. Title. II. Zarco, Mark A. III. Ebeling, Robert M. . U.S. Army Engineer Waterways Experiment Station. V. United States. Army. Corps of Engineers. VI. Technical report (U.S. Army Engineer Waterways Experiment Station) ; ITL-92-3.

TA7 W34 no.ITL-92-3